Supplemental Information 2:

TRACE document for *Population context matters: predicting the effects of metabolic stress mediated by food availability and predation with an agent- and energy budget-based model*

M.Vaugeois[1], Paul A. Venturelli[2], Stephanie L. Hummel[3], Chiara Accolla[1], and Valery E. Forbes[1]

[1]Department of Ecology, Evolution and Behavior, University of Minnesota, St. Paul, Minnesota, USA
[2]Department of Biology, Ball State University, Muncie, Indiana, USA
[3]US Fish & Wildlife Service, Bloomington, Minnesota, USA

This is a TRACE document ("TRAnsparent and Comprehensive model Evaludation"), which provides supporting evidence that our model presented in:

> **Vaugeois M., Venturelli P. A., Hummel S. L., Accolla C. and Forbes V. E., 2020: Population context matters: predicting the effects of metabolic stress mediated by food availability and predation with an agent- and energy budget-based model.**

was thoughtfully designed, correctly implemented, thoroughly tested, well understood, and appropriately used for its intended purpose.
The rationale of this document is as follows:

> Schmolke A, Thorbek P, DeAngelis DL, Grimm V. 2010. Ecological modelling supporting environmental decision making: a strategy for the future. *Trends in Ecology and Evolution* 25: 479-486.

and uses the updated standard terminology and document structure in:

> Grimm V, Augusiak J, Focks A, Frank B, Gabsi F, Johnston ASA, Kułakowska K, Liu C, Martin BT, Meli M, Radchuk V, Schmolke A, Thorbek P, Railsback SF. 2014. Towards better modelling and decision support: documenting model development, testing, and analysis using TRACE. *Ecological Modelling*

and

> Augusiak J, Van den Brink PJ, Grimm V. 2014. Merging validation and evaluation of ecological models to 'evaludation': a review of terminology and a practical approach. *Ecological Modelling*.

Contents

1 Problem formulation

This TRACE element provides supporting information on the decision-making context in which the model will be used; the types of model clients or stakeholders addressed; a precise specification of the question(s) that should be answered with the model, including a specification of necessary model outputs; and a statement of the domain of applicability of the model, including the extent of acceptable extrapolations.

The model that we present in this document aims to investigate the population-level impacts of a hypothetical, sublethal stressor that can affect an individual's metabolism (growth, reproduction, maintenance, or assimilation) in systems in which population size is controlled by different combinations of food availability and predation pressure. The life cycle of fathead minnow *Pimephales promelas* is described through their metabolism, using the Dynamic Energy Budget theory (DEB, Kooijman (2010)) and we represent the populations through an individual-based model.

Population effects of stressors, such as toxic chemicals or increased temperatures, affecting the energy budgets of organisms are mediated by predation pressure and food availability. So far, however, these two population contexts are mostly considered separately. Moreover, it is hard to predict combined stressor effects because the sensitivity of the different pathways of energy to stress may differ. The goals of this study were to link individual-level effects to population-level effects; evaluate population-level effects in different population dynamics contexts (top-down or bottom-up controlled systems); and evaluate differences at the population-level for different stressors' individual-level metabolic pathways (effects on growth, reproduction, maintenance, or assimilation).

2 Overview, Design concepts, Details

This TRACE element provides supporting information on the model. It provides a detailed written model description. The ODD protocol is recommended as a standard format for individual/agent-based models and other simulation models. For complex submodels, it should include concise explanations of the underlying rationale. Model users should learn what the model is, how it works, and what guided its design.

Summary:

Here we present the complete model description following the ODD (Overview, Design concepts, Details) designed for describing individual-based models.

The model description follows the ODD protocol (Grimm et al. (2006, 2010)). The model uses a DEB-IBM approach (Martin et al., 2012) and is developed in Java using the "SimAquaLife" framework (Dumoulin, 2007), which is an individual-based, process-oriented framework for simulating aquatic life. The code is publicly available at thttp://hdl.handle.net/11299/206495.

2.1 Purpose

The purpose of this model is to predict the population-level effects of exposure to stressors in different ecosystem contexts. We simulated stressor impacts at the individual level via four types of Physiological Modes of Action (PMoAs) (Álvarez et al., 2006; Jager and Zimmer, 2012): an increase in the cost of growth, an increase in the cost of reproduction, an increase in maintenance costs, and a decrease in assimilation rate.

2.2 Entities, state variables, and scales

There are two types of entities in the model: individual fish and spatial units. We used the scaled version of the Dynamic Energy Budget (DEB) model with metabolic acceleration to represent the energy budget of individuals. Individuals are characterized by six state variables (Table SI-2.0): structure (L, in cm); scaled reserve (U_E, in $d.cm^2$); scaled maturity (U_H, $d.cm^2$); scaled reproduction (U_R, $d.cm^2$); damage-inducing compounds ($\ddot{q}$), expressed as the aging acceleration; and damage ($\dot{h}$), expressed as hazard rate. For more details and introduction to Dynamic Energy Budget theory, see

van der Meer (2006); Nisbet et al. (2000); Sousa et al. (2010); Jusup et al. (2016).

The aging of individuals follows Martin et al. (2012). Briefly, aging in DEB theory is based on the idea that damage-inducing compounds (*i.e.*, free radicals) cause irreversible damage to DNA, and that the probability of dying by aging is proportional to the amount of damage. Aging is therefore described in terms of the state variables damage-inducing compounds ($\ddot{q}$), and damage ($\dot{h}$).

We accounted for inter-individual variability in parameter values by introducing a normally distributed number ($\mu = 1$ and $\sigma = 0.05$), the scatter multiplier, which impacts four of the eight standard DEB parameters (Table SI-2.0).

Table SI-2.0: State variables of the scaled DEB model.

Name	Notation	Dimension
Volumetric structural length	L	cm
Scaled reserve	U_E	$d.cm^2$
Scaled maturity	U_H	$d.cm^2$
Scaled reproduction	U_R	$d.cm^2$
Aging acceleration	$\ddot{q}$	d^{-2}
Hazard rate	$\dot{h}$	d^{-1}
Prey density	X	$J.cm^{-2}$

The number and size of spatial units is modular. In the present version, the model has one spatial unit representing a single 0.1 hectare zone of a river. When multiple spatial units are represented, individuals choose to move upstream or downstream or to stay in their current zone with an equal probability (see 2.3).

A zone is characterized by 3 quantitative state variables: prey density (X, $J.cm^{-2}$), temperature (T, in C) and surface area (in m^2). Prey density changes daily (*i.e.*, at each time step) and independently in each zone according to a logistic growth function and what is consumed by fishes in the zone. The logistic growth function has two parameters: intrinsic growth rate (denoted a_E, with dimension d^{-1}) and carrying capacity (denoted k_E, with dimension $J.m^{-2}$). Temperature is the same in all zones and changes daily according to seasonally varying temperature data that were recorded in 2015 in the Kawishiwi River, MN (range from 0.9 to 24.4 °C), and downloaded from the USGS website (https://waterdata.usgs.gov/nwis).

Model integration is done following the classical Runge-Kutta method using the Apache Commons Math library (release 3). One time step represents one day, and simulations are run for 20 years. Exposure to a stressor, if present, starts at 15 years.

Table SI-2.0: Parameters of the scaled abj DEB model for *Pimephales promelas*. *wd* stands for without dimensions.

Name	Notation	Value	Dimension
Standard parameters			
Fraction of mobilized energy to soma	κ	0.481	wd
Fraction of reproduction energy fixed in eggs	κ_R	0.95	wd
Somatic maintenance rate coefficient	$\dot{k}_M$	0.026	d^{-1}
Maturity maintenance rate coefficient	$\dot{k}_J$	0.002	d^{-1}
Scaled maturity at hatching	U_H^h	0.4835	$d.cm^2$
Scaled maturity at birth	U_H^b	0.722	$d.cm^2$
Scaled maturity at metamorphosis for female	U_H^j	2.941	$d.cm^2$
Scaled maturity at puberty for female	U_H^p	3432	$d.cm^2$
Scaled maturity at metamorphosis for male	U_H^{jm}	4.927	$d.cm^2$
Scaled maturity at puberty for male	U_H^{pm}	3491	$d.cm^2$
Energy conductance	$\dot{v}$	0.01921	$cm.d^{-1}$
Energy investment ratio	g	1.174	wd
Ageing parameters			
Weibull aging acceleration	$\ddot{h}_a$	1.158e-8	d^{-2}
Gompertz stress coefficient	S_G	0.0001	wd
Auxiliary parameters			
Digestion efficiency of food to reserve	κ_X	0.8	wd
Chemical potential of reserve	μ_X	550000	mol^{-1}
Surface area-specific maximum ingestion rate	$\{J_{XAm}\}$	4.042e-4	$L^{-2}t^{-1}$
Surface-area-specific searching rate rate	$\{F_m\}$	6.5	$\mathrm{l}\cdot\mathrm{cm}^{-2}\cdot\mathrm{d}^{-1}$
Arrhenius temperature	T_A	8000	K
Reference temperature	T_{ref}	293.15	K

2.3 Process overview and scheduling

The model executes the following actions at each time step. First, individuals are listed by zone. Individuals in each zone then update their DEB state variables. This update can result in three

forms of mortality: starvation (*i.e.*, an inability to pay maintenance costs, aging, or predation (stage-dependent survival rate to predation). Starvation is deterministic (*i.e.*, depends on a state variable), and death by aging and predation are stochastic (*i.e.*, depend on random selection). Both starvation death and death by aging are based on individual energetics and interactions with the environment. Predation is a stage-dependent, external cause of death.

Reproduction occurs after updating the DEB state variables of each individual. Only adults with a minimum amount of energy allocated to reproduction (UR, $d.cm$) are able to reproduce. Females can only reproduce if they share a zone with a male that is also ready to reproduce.

2.4 Design concepts

2.4.1 Basic principles

The model is based on Dynamic Energy Budget theory for describing the energetics of individuals. The DEB model describes how individuals feed, allocate energy for growth and reproduction, and die of aging, predation, and/or starvation. Food in our model is limited by both fish density and the logistic growth parameter of food defined in spatial units. DEB theory allows for the representation of two kinds of mortality: aging and starvation. We also introduced mortality due to predation. Because the goal of this model was to estimate the population-level effects of exposure to stressors with different PMoA in different river system types, we parametrized the model for different system types (see 3.2.1).

2.4.2 Emergence

The following variables emerge from the behavior of individuals, their metabolism, the indirect interactions of individuals through competition for food, and predation: fish population density, the average number of reproduction events per female, the average spawning interval, and the Fulton condition index (Shin et al., 2005) (*i.e.*, ratio of weight to cubic length).

2.4.3 Adaptation

The model does not contain adaptive behavior. DEB parameters differ among individuals, but they stay constant over the simulation of each individual. The model is also free of evolutionary adaptation;

parameter values for new individuals in the model are set identically as in the initialization process (see 2.5).

2.4.4 Objectives

The objective of this model was to compare population-level impacts of different individual-level responses to stressors in different ecosystem types. Therefore, we modeled a river environment with two controlling variables: food availability and stage-dependent predation. Stage-dependent probabilities of dying from predation are constant throughout the simulations. Several simulations were run with different sets of parameters for food logistic growth and stage-dependent survival rates in response to predation. We analyzed the outputs to determine the conditions (*i.e.*, set of parameters) under which a realistic population pattern is observed (for more details, see section 3.2.1).

2.4.5 Learning

There is no learning process in the model.

2.4.6 Prediction

There is no prediction in the model.

2.4.7 Sensing

There is no Sensing process in the model.

2.4.8 Interactions

Individuals interact directly via reproduction, and indirectly via competition for food.

2.4.9 Stochasticity

Some DEB parameters vary among individuals. We followed the same methodology as Martin et al. (2012), based on Kooijman et al. (1989), to set variability among individuals. Briefly, the surface area specific maximum ingestion rate $\{\dot{J}_{XAm}\}$ is multiplied by a scatter multiplier to introduce differences

between individuals. It impacts six DEB parameters: the half-saturation coefficient K which is multiplied by the scatter multiplier; the energy investment ratio g, which is divided by the scatter multiplier because it equals $\frac{[E_G]\dot{v}}{\kappa\{\dot{P}_{Am}\}}$, with $\{\dot{P}_{Am}\} = \{\dot{J}_{XAm}\}\kappa_X\mu_X$; and the scaled maturity thresholds for hatching U_H^h, birth U_H^b, metamorphosis U_H^j and puberty U_H^p, which are divided by the scatter multiplier because we use the scaled DEB model (which is the standard DEB model scaled by $\{\dot{P}_{Am}\}$, see (Kooijman et al., 2008) for more details on scaling the standard DEB model).

Other sources of stochasticity include the order in which organisms are updated, the random selection of individuals at each time step by zone, and the probabilities of dying by aging or predation.

We assign a seed value to each simulation replicate of the same conditions. This allowed us to have the same level of stochasticity when comparing simulations having different conditions.

2.4.10 Collectives

There is no aggregation behavior in the model.

2.4.11 Observations

We collected observations on fish density, eggs per reproductive event per female, mean time between two reproductive events (spawning interval) for females, mean individual size (length and weight), the Fulton condition index (ratio of weight to cubic length), total biomass, and Population Size Distribution (PSD, ratio of the number of individuals $\geq$ 4.5cm over the number of individuals $\geq$ 1.5cm).

2.5 Initialization

Food density is set to carrying capacity in all zones at the beginning of each simulation.

All simulations began with a 4-year phase-in period that involved introducing new individuals during each reproductive season (Andrews and Flickinger, 1974).

We introduced variability among individuals as described in section 2.4.9. The initial set of DEB parameters (*i.e.*, the one on which we apply a scatter multiplier) is the one from the parameterization of the individual DEB model (Lika et al., 2011). The initial values of the DEB state variables are $L = 0.001$, $U_R = 0$, and $U_H = 0$. The initial amount of scaled reserve U_E is calculated for each

individual using the bisection method from Martin et al. (2012). Briefly, this method determines the initial amount of scaled reserve via adaptive trial and error so that the reserve density (E/V) of the offspring at birth is similar to the reserve density of the mother when she produces the offspring.

2.6 Input data

The model uses a single year of daily water temperature data for all zones and years. These data were recorded in 2015 in the Kawishiwi River, MN , and can be downloaded from the USGS website (https://waterdata.usgs.gov/nwis).

Table SI-2.0: Equations of the scaled abj DEB model for ectotherms.

Differential equations
$\frac{\mathrm{d}U_E}{\mathrm{d}t} = S_A - S_C$
$\frac{\mathrm{d}L}{\mathrm{d}t} = \frac{1}{3}\left(\frac{\dot{v}S_C}{gL^2} - \dot{k}_M L\right)$
$\frac{\mathrm{d}U_H}{\mathrm{d}t} = (1-\kappa)S_C - S_J$ if $U_H < U_H^p$, else $\frac{\mathrm{d}U_H}{\mathrm{d}t} = 0$
$\frac{\mathrm{d}U_R}{\mathrm{d}t} = 0$ if $U_H < U_H^p$, else $\frac{\mathrm{d}U_R}{\mathrm{d}t} = (1-\kappa)S_C - S_J$
$\frac{\mathrm{d}\ddot{q}}{\mathrm{d}t} = \left(\ddot{q}\left(\frac{L}{L_m}\right)^3 s_G + h_a\right)e\left(\frac{v}{L} - \frac{3}{L}dL\right) - \frac{3}{L}dL\ddot{q}$ with $L_m = \frac{\dot{v}}{\dot{k}_M * g}$
$\frac{\mathrm{d}\dot{h}}{\mathrm{d}t} = \ddot{q} - \frac{3}{L}dL\dot{h}.$
Fluxes equations
$S_A = c(T)f(X)L^2$ if $U_H \geq U_H^b$, else $S_A = 0$
$S_C = c(T)L^2\frac{ge}{g+e}\left(1 + \frac{L\dot{k}_M}{\dot{v}}\right)$; with $e = \frac{E}{E_m}$, $g = \frac{[E_G]}{\kappa[E_m]}$, and $[E_m] = \frac{\{\dot{P}_{Am}\}}{\dot{v}}$
$S_J = c(T)\dot{k}_J U_H$
Scaled food and temperature functions
$f(X) = \frac{X}{X+K}$, with $K = \frac{\{\dot{J}_{XAm}\}\mu_X}{\{\dot{F}_m\}}$
$c(T) = exp\left(\frac{T_A}{T_{ref}} - \frac{T_A}{T}\right)$

2.7 Sub-models

The model includes two sub-models: the DEB sub-model, which includes DEB state variables (updated daily), death due to starvation, death due to aging, death due to predation, and prey dynamics; The reproduction sub-model describes when individuals reproduce and how they accordingly update the corresponding state variables.

2.7.1 DEB sub model

- For each individual in the zone:
  - Calculate the change in reserve due to feeding and mobilized energy.
  - If maturity is less than the maturity threshold for puberty, then calculate the change in maturity. Otherwise, calculate the change in reproduction buffer.
  - Calculate the change in length.
  - If the change in length is less than 0, then recalculate structure, reserves, maturity, and reproduction buffer based on starvation rules (see section 2.8).
  - Calculate the change in aging acceleration and hazard based on aging (*i.e.*, the probability of dying due to aging, see section 2.10).
  - Calculate the change in prey density based on feeding (see section 2.9).
  - Update the DEB state variables.
  - If a randomly selected number (continuous uniform distribution U(0,1)) is less than the probability of dying from aging, then die. The probability of dying from aging at a moment t is $1 - H$, where H is the integral from 0 to t of $\dot{h}$.
  - If a randomly selected number (continuous uniform distribution U(0,1)) is less than the probability of dying from predation, then die. The probability of dying from predation is stage-dependent and is calculated from the parameter: annual, stage-dependent probability of survival from predation. The annual egg survival rate was fixed to 0.025 (*i.e.*, equivalent to a survival rate of 0.96 to 0.95 for a 4 to 5 day long egg stage) according to the hatching rate in Ankley et al. (2001). The annual larvae survival rate was fixed to $2.57\ 10^{-49}$ (*i.e.*,

equivalent to a survival rate of 0.74 to 0.54 for a 1 to 2 day long larval stage) according to the larval survival rate in a predation trial in Korn (2018). Juvenile and adult survival rates were fixed for each system but vary from one system to another.

- Update prey density for the zone after all individuals have been updated (see section 2.9).

2.7.2 Reproduction sub-model

- If the environmental temperature is >15°C:
  - List all individuals that are ready to reproduce (*i.e.*, reproduction buffer is greater than the threshold for reproduction, see section 2.11).
  - Allow reproduction among all females that are ready to reproduce and sharing a zone with at least one male that is also ready to reproduce. As the time step is daily, both males and females reproduce once a day at maximum:
    * calculate the initial amount of energy in eggs.
    * calculate number of fertilized eggs spawned and update female reproduction buffer accordingly (see section 2.11).
    * randomly select a male among the ready to reproduce males.
    * calculate the amount of energy needed for the reproduction event for the male (set as the energy equivalent for producing two eggs for the female) and update the male reproduction buffer.
    * create new female individuals by setting the number of new females to half the number of fertilized eggs spawned (ceiling function, sex ratio 1:1). The initial amount of energy is calculated based on reserve density of the mother using the bisection method. The parameter values for each new individual are set as in the initialization.
    * create male individuals by setting the number of new males to half the number fertilized eggs spawned (flooring function, sex ratio 1:1). Rules for parameter values and initial amount of energy are the same as for females.

2.8 Starvation

Individuals interact indirectly through competition for a limited food resource. Some individuals die of starvation as a result of this competition. Although many starvation strategies can be implemented with DEB theory (Kooijman, 2010; Martin et al., 2012), we implemented the following strategy because it is the most realistic for fish.

DEB theory specifies that organisms use energy to grow and reproduce based on available energy in the reserve compartment. This reserve compartment is fueled by the assimilation process. When food is scarce, the assimilation flux is weakened, and the energy content of the reserve compartment may be insufficient for growth, maintenance, and reproduction/maturation. Individuals enter starvation when they cannot pay their maintenance cost (*i.e.*, when $[E]/[E_m] < L/L_m$). Growth is no longer possible at this point (dL/dt = 0), and somatic maintenance is prioritized. If the organism has not reached puberty, then its level of maturity may decrease, otherwise available energy for reproduction may decrease. When the reserve is empty and, for non-adults, if maturity decreases to 0, then the organism dies. If the mobilized energy is less than the energy needed for maintenance, then the organism dies.

2.9 Prey density update

Resource density, X ($J.m^{-2}$), is modeled as a generic logistic function.

$$\frac{\mathrm{d}X}{\mathrm{d}t} = c(T)a_E X\left(1 - \frac{X}{K_E}\right)$$

were a_E ($J.J^{-1}.d^{-1}$) is intrinsic growth rate and K_E ($J.m^{-2}$) is carrying capacity. The resource density is updated after each individual eats in a time step. The amount of food that an individual eats is determined by its energetic parameters. We prevented the total depletion of food by introducing a lower resource density below which individuals cannot feed. We fixed this value to eight times the individual half saturation coefficient ($K = \frac{\{\dot{J}_{XAm}\}\mu_X}{\{\dot{F}_m\}}$). The resource density is updated according to the logistic function after all individuals have eaten in a time step.

2.10 Aging

The aging process is described in DEB theory as the consequence of irreparable damage caused by free radicals or related reactive oxygen species (ROS). These damage-inducing compounds accumulate at a rate that is proportional to the mobilization rate, and the probability of dying is proportional to the amount of damage that is induced. The two state variables that describe aging mortality are thus the acceleration at which damage-inducing compounds accumulate, $\ddot{q}$ $[t^{-2}]$, and the hazard or death rate $\dot{h}$ $[t^{-1}]$, proportional to the damage density. The differential equations for these two variables can be found in table 3.1. The integral of $\dot{h}$ over time gives the conditional probability of dying at time $t + \Delta t$ given that an organism has survived up to t. The survival probability is calculated from the hazard rate as follows (Kooijman, 2010):

$$\frac{\mathrm{d}Pr(a > t)}{\mathrm{d}t} = -Pr(a > t)\dot{h}(t),$$

where a is the age of death of the organism. Therefore, the survival function at time t is:

$$R(t) = \exp^{-\int_0^t \dot{h}(\xi)d\xi}.$$

The mortality probability at t is calculated as $m(t) = 1 - R(t)$.

2.11 Reproduction

We introduced a calibrated parameter ($R_{Threshold} = 27.018$) so that individuals were deemed ready to reproduce when $U_R/L^3 \geq R_{Threshold}$.

In our model, a female can use only a fixed percent of reproductive buffer, U_R, per reproductive event. This percent was calibrated to allow each female to spawn several times during the reproductive season.

The number of fertilized eggs is calculated from the number of spawned eggs, as follows:

$$NB_{E_F} = FR \cdot 0.12 \cdot U_R/\kappa_R$$

where FR is the proportion of fertilized eggs, calculated as a function of temperature according to fertilization rates at different temperatures in Ward et al. (2017):

$$FR = aT + b,$$

where T is environmental temperature and a (0.01613) and b (0.38204) are the two coefficients of this function. We ensured that FR was smaller than 1 at the maximum temperature value that we used.

2.12 Effects of stressors

We modeled only sub-lethal effects of stressors as effects on different PMoAs. We considered stressor effects on one PMoA at a time as follows with a stress parameter s ($0 < s \leq 1$):

- Feeding: $f = f * (1 - s)$
- Maintenance: $K_M = K_M(1 + s); K_J = K_J(1 + s)$
- Growth: $K_M = K_M(1 + s); g = g * (1 + s)$
- Reproduction: $\kappa_R = \kappa_R * (1 - s)$

2.13 Shape and temperature corrections

Two corrections are needed to account for metabolic acceleration and the effects of temperature. The first correction is the multiplication by the *shape correction* function (sc). This function is equal to 1 for isomorph organisms, which are those individuals that do not change their shape during growth. Their surface is proportional to their volume to the power of 2/3 ($V^{2/3}$). On the contrary, if shape changes during growth, then two other morphisms are possible: V0-morphs (surface area proportional to V^0) and V1-morphs (surface proportional to V^1). Fish have a unique life cycle, and their growth shows an acceleration during a short period of time, between birth and puberty (called "metamorphosis" in DEB theory). During this time, they are considered as V1-morphs. From a mathematical point of view, this translates into a slight modification of DEB theory by multiplying the maximum specific assimilation rate ($\{\dot{p}_{Am}\}$), the specific searching rate ($\{\dot{F}_m\}$), the specific surface area-linked somatic

maintenance rate ($\{\dot{p}_T\}$, equal to 0 in our model) and the energy conductance ($\dot{v}$) by sc.

$$
\begin{aligned}
sc &= 1 \quad if \quad U_H < U_H^b \\
sc &= \frac{L}{L_b} \quad if \quad U_H^b \leq U_H < U_H^j \\
sc &= \frac{L_j}{L_b} \quad if \quad U_H \geq U_H^j
\end{aligned}
$$

L_b and L_j are the lengths at birth and metamorphosis. In our code, this means that we have to multiply $\{\dot{J}_{XAm}\}$, $\{\dot{F}_m\}$, $\dot{v}$, S_A and S_C by the sc factor.

The second modification is the multiplication of the assimilation rate by the correction for temperature, T_{corr}. Every energy flow is influenced by this modification because temperature affects all metabolic rates. In our code, this means that dU_E, dU_H, dU_R, dL, $d\ddot{q}$, $d\dot{h}$ are multiplied by the temperature correction factor.

3 Data evaluation

This TRACE element provides supporting information on: The quality and sources of numerical and qualitative data used to parameterize the model, both directly and inversely via calibration, and of the observed patterns that were used to design the overall model structure. This critical evaluation will allow model users to assess the scope and the uncertainty of the data and knowledge on which the model is based.

Summary:

Here we provide information on the type of data that were used to parameterize the individual properties. This pertains mostly to the parameterization of the DEB model. The parameters related to population properties are fairly uncertain, and model results are sensitive to them. They were calibrated to represent demographic patterns found in the literature.

3.1 DEB parameterization

This section presents a model representing the full life cycle of *Pimephales promelas*. This model describes the growth, reproduction and maintenance at the individual scale based on the Dynamic Energy Budget (DEB) theory (Kooijman, 2010). It is a DEB model with type M acceleration, which means that metabolism accelerates during a part of the life cycle. This model is a one-parameter extension of standard DEB model.

This section is organized as follows: First, we briefly describe the standard DEB model and the type M acceleration. Then we briefly introduce the parameter estimation method that was used in this work. Finally, we present the data used in this parameter estimation, and provide a comparison of the model outputs and empirical data.

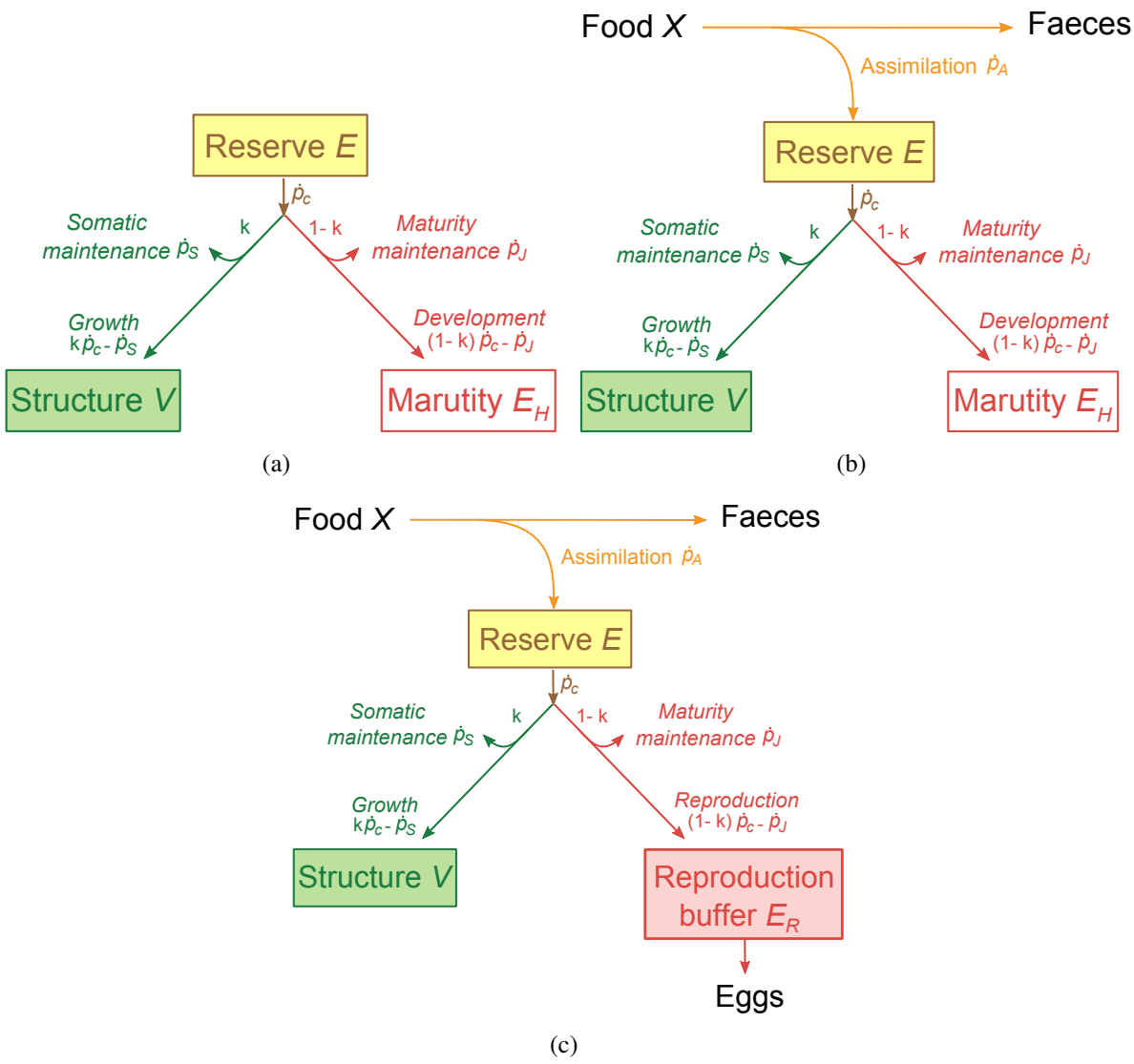

Figure SI-2.1: **Schematic representation of the three life stages of the standard DEB model.** (a) An embryo uses reserve to grow and develop. (b) At birth, a juvenile starts exogenous feeding, and (c) at puberty, an adult starts allocating energy to reproduction.

3.1.1 Methods

DEB model The standard DEB model describes the entire life cycle of an organism through three life stages. This paragraph gives a short presentation of DEB theory; see Kooijman (2010) for more details.

Here we introduce state variables and fluxes (Table 3.1) from a life cycle point of view. In DEB theory, life cycle is described in 3 stages and the transition between one stage to the next depends on

Table SI-2.1: Equations of the standard DEB model for ectotherms.

Differential equations
$\frac{\mathrm{d}}{\mathrm{d}t}E = \dot{p}_A - \dot{p}_C$
$\frac{\mathrm{d}}{\mathrm{d}t}V = \frac{1}{[E_G]}\dot{p}_G = \frac{1}{[E_G]}(\kappa\dot{p}_C - \dot{p}_S)$
$\frac{\mathrm{d}}{\mathrm{d}t}E_H = (1-\kappa)\dot{p}_C - \dot{p}_J$ if $E_H < E_H^p$, else $\frac{\mathrm{d}}{\mathrm{d}t}E_H = 0$
$\frac{\mathrm{d}}{\mathrm{d}t}E_R = 0$ if $E_H < E_H^p$, else $\frac{\mathrm{d}}{\mathrm{d}t}E_R = (1-\kappa)\dot{p}_C - \dot{p}_J$
Fluxes equations
$\dot{p}_A = c(T)f(X)\{\dot{p}_{Am}\}L^2$ if $E_H \geq E_H^b$, else $\dot{p}_A = 0$
$\dot{p}_C = c(T)\{\dot{p}_{Am}\}L^2\frac{ge}{g+e}\left(1 + \frac{L}{gL_m}\right)$; with $e = \frac{E}{E_m} = \frac{E}{V}\frac{\dot{v}}{\{\dot{p}_{Am}\}}$ and $L = V^{\frac{1}{3}}$
$\dot{p}_S = c(T)[\dot{p}_M]L^3$
$\dot{p}_J = c(T)\dot{k}_J E_H$
Scaled food and temperature functions
$f(X) = \frac{X}{X+K}$, with $K = \frac{\{\dot{J}_{XAm}\}\cdot\mu_X}{\{\dot{F}_m\}}$
$c(T) = exp\left(\frac{T_A}{T_{ref}} - \frac{T_A}{T}\right)$

a state variable, called maturity E_H.

The organism does not feed during the first (*i.e.*, embryonic) life stage, so the flux for assimilation $\dot{p}_A$ is zero. The organism uses the available energy in its reserve compartment (E), with a fixed allocation rate (κ), to grow in structure (V). A proportion κ of the mobilization flux $\dot{p}_C$ goes to the structure (V) for its maintenance $\dot{p}_S$ and its growth which thus equals $\kappa\dot{p}_C - \dot{p}_S$. What remains of the mobilization flux (*i.e.* $(1-\kappa)\dot{p}_C$) is allocated to maturity E_H for maintenance ($\dot{p}_J$) and maturity increase. The resultant increase in maturity is given by $(1-\kappa)\dot{p}_C - \dot{p}_J$. The maintenance of the structure ($\dot{p}_S$) depends on temperature through the Arrhenius relationship ($c(T)$), and also on its surface and/or volume. The maintenance of maturity depends on temperature, with the same Arrhenius relationship ($c(T)$), and on the amount of maturity.

The second stage is the juvenile stage. It begins when the organism is able to feed exogenously, *i.e.*, when maturity has reached a fixed threshold (E_H^b). Therefore, the assimilation flux $\dot{p}_A$ is no longer zero. The assimilation depends on temperature, environmental food condition ($f(X)$) and the

structural surface of the organism. The assimilated energy supplies the reserve compartment from which energy is allocated to growth or maturation, still with the same κ allocation rule.
The organism enters the adult stage when maturity has reached a fixed amount of energy (E_H^p). From this moment, named puberty, energy that was previously allocated to maturity is now allocated to reproduction. Nevertheless, maturity maintenance continues, and the allocation rate to growth or maturity/reproduction is still the same.

The metabolic acceleration occurs between birth and a moment defined as metamorphosis (when maturity reaches a threshold value (E_H^j), before puberty) which might or might not correspond with changes in morphology.

Parameter estimation The parameters of the standard DEB model were estimated using the co-variation method (Lika et al., 2011). This method uses the simplex method to simultaneously minimize the weighted sum of squared deviations between model predictions and observations for a considerable number of data sets. Two types of data are used: the uni-variate data and the zero-variate data. Uni-variate data consist of sets of time-series observations, like growth versus time. The zero-variate data are composed of pseudo-data and real-data. Pseudo data are parameter values that are supposed to be highly conserved among all the taxa, so that they serve as a kind of prior knowledge about the organism. Real data are empirical observations such as maximum length and weight at birth and/or puberty and/or death, lifetime, and number of eggs produced. A weight coefficient can be assigned to each uni-variate data set, and both kinds of zero-variate data set. We assigned the same weight to every data set in the present study.
We accounted for sexual dimorphism by introducing different values (and therefore new parameters) for some maturity thresholds. We introduced sex-specific thresholds for metamorphosis (E_H^{jm}) and puberty (E_H^{pm}) for males that have different values than females. Another way to account for sexual dimorphism is to introduce sex-specific zoom factors such that males and females have different maximum assimilation rate ($\{\dot{p}_{Am}\}$) and half-saturation ($K = \{\dot{J}_{XAm}\}\mu_X/\{\dot{F}_m\}$) coefficients. We did not opt for this solution for two reasons. First, we are unaware of any evidence that feeding rate is sex-specific in fathead minnows. Second, we do not want to introduce a sex difference in the ability to compete for food because we intend to use this DEB model to describe the energetics of agents in

an Individual Based Model.

Table SI-2.1: Parameters for *Pimephales promelas*, state variables and forcing variables of the standard DEB model.

Symbol	Value	Units	Definition
		State and forcing variables	
E		J	Reserve density
V		cm^3	Structural volume
E_H		J	Cumulated energy invested into development
E_R		J	Reproduction buffer energy
X		$J \cdot l^{-1}$	Food density
T		K	Temperature
$f(X)$			Scaled functional response
$c(T)$			Temperature correction factor
		Primary parameters	
$[\dot{p}_M]$	133.5	$J \cdot cm^{-3} \cdot d^{-1}$	Volume-specific somatic maintenance rate
$\{\dot{p}_T\}$	0	$J \cdot cm^{-2} \cdot d^{-1}$	Surface-area-specific somatic maintenance rate
$[E_G]$	5228	$J \cdot cm^{-3}$	Volume-specific cost for structure
$\dot{v}$	0.01921	$cm \cdot d^{-1}$	Energy conductance
κ	0.481		Fraction reserve used for growth + maintenance
$\dot{k}_J$	0.0020	d^{-1}	Maturity maintenance rate coefficient
E_H^h	0.4835	J	Maturity threshold at hatching
E_H^b	0.722	J	Maturity threshold at birth
E_H^j	2.941	J	Maturity threshold at metamorphosis
E_H^{jm}	4.927	J	Maturity threshold at metamorphosis for male
E_H^p	3432	J	Maturity threshold at puberty
E_H^{pm}	3491	J	Maturity threshold at puberty for male
κ_R	0.95		Fraction of the reproduction buffer fixed into eggs
$\{F_m\}$	6.5	$l \cdot cm^{-2} \cdot d^{-1}$	Surface-area-specific searching rate rate
		Auxiliary and compound parameters	
κ_X	0.8		Digestion efficiency of food to reserve
T_A	8000	K	Arrhenius temperature
T_{ref}	293.15	K	Temperature
δ_M	0.1268		Shape coefficient
z	0.6408		Zoom factor
s_G	0.0001		Gompertz stress coefficient
h_a	1.158e-08	$l.d^{-2}$	Weibull aging acceleration

3.1.2 Results

We used a previously developed version of a DEB model for *Pimephales promelas*[1]. We modified some zero-variate data and added some new data in order to model both female and male fathead minnows (Table SI-2.1).

We also added uni-variate data on length and weight both for females (Fig. SI-2.2) and males (Fig. SI-2.3). These data were extracted from experiments performed at Saint-Cloud State University (SCSU - Heiko Schoenfuss Lab, personal communication).

Table SI-2.1: Real versus estimated data values used for parameter estimation of DEB model for *Pimephales promelas*. RE is the relative error.

Data (dimension)	Value	Source	Modeled	RE
Age at hatching (d)	4.5	Braunbeck et al. (1998); Jeffries et al. (2015)	4.801	0.06699
Age at hatching at 15 °C (d)	13	Sommer (2011)	12.18	0.06279
Age at birth (d)	6	Sommer (2011)	5.926	0.01232
Age at puberty for female (d)	135	Sommer (2011)	133.7	0.009699
Age at puberty for male (d)	135	Sommer (2011)	111.9	0.171
Age at death (d)	1460	Sommer (2011)	1460	6.342e-09
Wet weight at birth (10^{-4} g)	3.393	Braunbeck et al. (1998)	3.602	0.0003602
Wet weight at puberty for female (g)	0.7857	Braunbeck et al. (1998)	0.7371	0.06182
Wet weight at puberty for male (g)	0.7857	Braunbeck et al. (1998)	0.8514	0.08356
Wet weight at death for female (g)	3	Sommer (2011)	3.077	0.02574
Wet weight at death for male (g)	5	Sommer (2011)	5.123	0.02461
Length at birth (cm)	0.5	Wang (1986)	0.3884	0.2231
Length at puberty for female (cm)	4	Braunbeck et al. (1998)	4.931	0.2329
Length at puberty for male (cm)	5	Braunbeck et al. (1998)	5.174	0.03482
Length at death for female (cm)	8.09	Collected from Lab data from SCSU	7.941	0.01847
Length at death for male (cm)	10.1	Etnier and Starnes (1993)	9.411	0.06821
Number of egg per day ($\#/d$)	34	Watanabe et al. (2007)	33.12	0.02599

Zero-variate data (Table SI-2.1) are accurately reproduced by the model. The modeled ages at puberty at 25 and 15 °C are respectively 4.8 and 12.2 days, which is consistent with the observed values (4.5 and 13 days, respectively). Age at birth is also accurately modeled with a value of 5.93 days for an observed value of 6 days. There is no difference in age at puberty between the two sexes reported in the literature. Nevertheless, the reported range of variation is between 4 and 5 months. The modeled value of puberty for males is 111.9 days, which is slightly lower than 4 months ; and the modeled value of puberty for females is about 3.5 months (133.7 days). Age at death is the same for both males and females, and the modeled value is identical to the observed value (1460 days).

[1] `https://www.bio.vu.nl/thb/deb/deblab/add_my_pet/entries_web/Pimephales_promelas/Pimephales_promelas_res.html` - version of 2011/03/17.

Modeled weight at birth is the same for both sexes (3.6010⁻4 g), and is in accordance with the measured value (3.3910⁻4 g). Modeled weight at puberty is different for females (0.74 g) and males (0.85g), and both are close to the observed value (0.79 g). Modeled maximum weights for females (3.08 g) and males (5.12 g) are in accordance with reported literature data (3 and 5 g, respectively). Modeled length at birth (0.39 cm) is lower than observed (0.5 cm). Modeled length at puberty is overestimated for females (modeled 4.93 cm versus 4 cm reported), but in accordance with literature for males (modeled 5.17 cm versus 5 cm reported). Modeled maximum lengths for females (7.94 cm) and males (9.41 cm) are in accordance with literature data (8.09 and 10.1 cm, respectively). Finally, the number of eggs per day modeled (33.12) is similar to observed eggs per day (34).

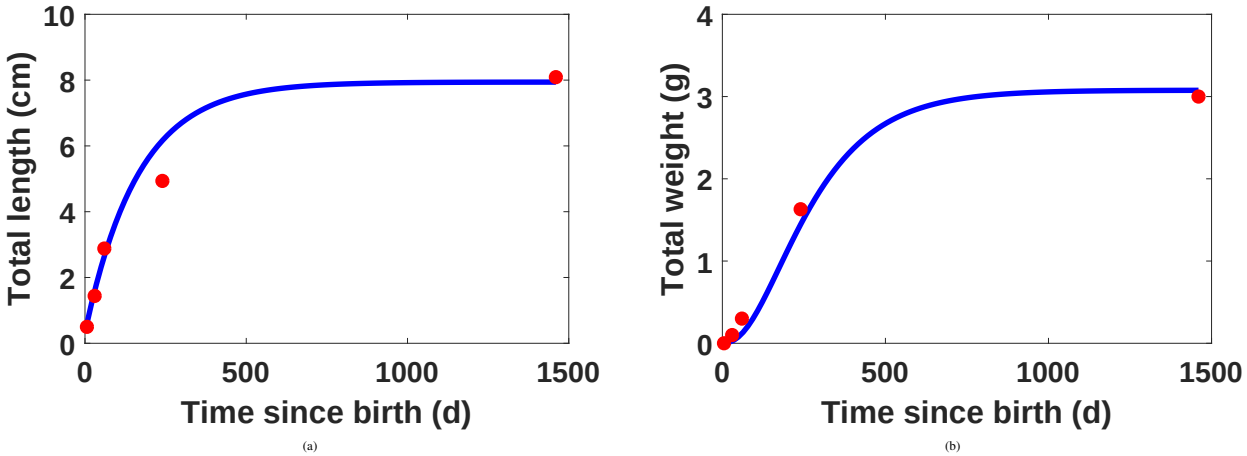

Figure SI-2.2: Model outputs versus length data (a) and wet weight data (b) for female *Pimephales promelas*. Blue lines show model output, and represent the result of one simulation of the DEB model with the best set of parameters that was estimated. Red dots are empirical data from Saint-Cloud State University (extracted data from experiments published in Ward et al. (2017); Cox et al. (2018)). Relative error was 0.1044 for length prediction and 0.1052 for wet weight prediction.

Uni-variate data are accurately reproduced by the model (Fig. SI-2.2 and SI-2.3). Part of the growth curves are missing because we could only access length and weight data for juveniles, young adults and late adults. Nevertheless, even if the modeled length at 300 days is overestimated, both female length (Fig. 6(a)) and weight (Fig. 6(b)) are accurately simulated for the whole life cycle. Male growth in length (Fig. 3(a)) and weight (Fig. 3(b)) are also accurately modeled when compared with collected data. For both males and females, the shapes of the modeled growth curves in early developmental stages realistically reproduced the patterns observed in the data. The maximum values for lengths and weights are in accordance with the data, and the onsets of the plateau seem realistic

given that wild adults, with life expectancies ranging from 2 to 3 years old, are reported in the literature with similar sizes (Sommer, 2011).

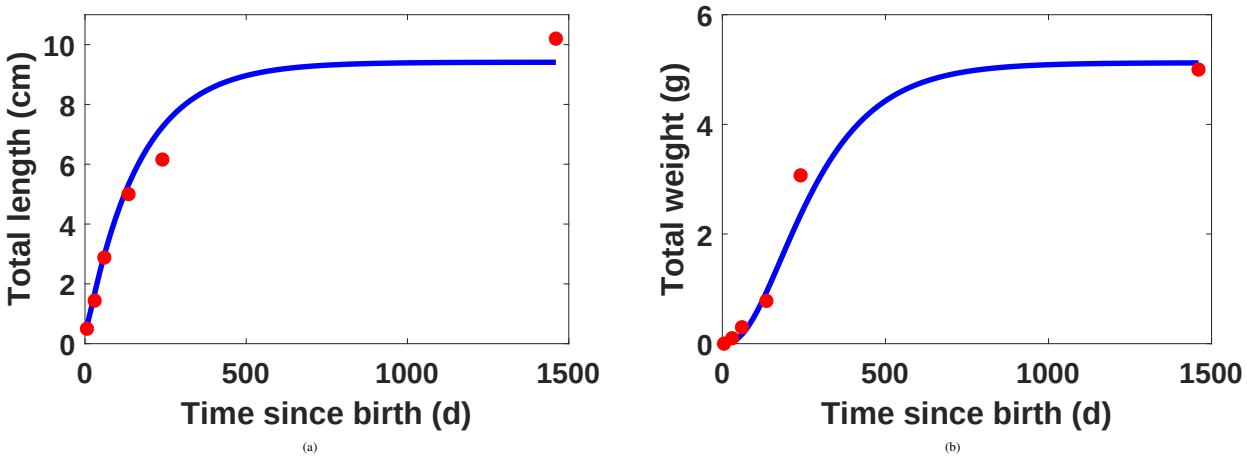

Figure SI-2.3: Model outputs versus length data (a) and wet weight data (b) for male *Pimephales promelas*. Blue lines are model output, and represent the result of one simulation of the DEB model with the best set of parameters that was estimated. Red dots are empirical data from Saint-Cloud State University (extracted data from experiments published in Ward et al. (2017); Cox et al. (2018)). Relative error was 0.1005 for length prediction and 0.1307 for wet weight prediction.

Another parameterization version for *Pimephales promelas* was performed recently (Stadnicka et al., 2018) and is available on-line [2]. This parameterization was done with more uni-variate data than ours, but with a comparable amount of zero-variate data.

There are some differences in the parameter values between our estimation and Stadnicka et al. (2018) (Table SI-2.3). The most important are for κ (0.48 versus 0.93), $\dot{v}$ (0.019 versus 0.042), δ_M (0.13 versus 0.21) and $[P_M]$ (133.5 versus 334.8).

Differences in some parameter values resulted in differences in some life history traits (Table SI-2.3). Virtual fish from Stadnicka et al. (2018) are smaller in length at birth (0.36 versus 0.39cm), at puberty (3.99 cm versus 4.93 cm), and at death (5.43 cm versus 7.94 cm for females ; 7.28 cm versus 9.41 cm for males). They are also smaller in weight at the adult stage (2.04 g versus 3.08 g at death for females ; 4.93 g versus 5.12 g at death for males) but they are bigger otherwise (0.81 g versus 0.74 g at puberty ; 6.22 10^{-4} g versus 3.55 10^{-4} g at birth). Regarding other aspects, virtual fish from Stadnicka et al. (2018) reproduce less (12.53 versus 33.12 eggs per day) but live longer (1821 days versus 1460 days) and mature earlier (birth at 5.07 days and puberty at 90.12 days versus 5.93 and 133 for females and

[2] `https://www.bio.vu.nl/thb/deb/deblab/add_my_pet/entries_web/Pimephales_promelas/Pimephales_promelas_res.html` - This new version has erased the previous one we referred to above.

111.9 days for males).

3.1.3 Conclusions

The DEB model calibrated for *Pimephales promelas* provides an accurate representation of the full life-cycle in different simulation contexts both for male and female individuals, which guarantees that the DEB model estimations are in accordance with reality.

Life-cycle events (*i.e.* ages at hatching, birth, puberty, death) at different temperatures are well estimated. Lengths and weights observed at each of these life-cycle events, as well as the reproduction rate, are also well reproduced by the model.

Pimephales promelas exhibits a sexual dimorphism that is taken into account by the DEB model. Female (Fig. SI-2.2) and male (Fig. SI-2.3) growth patterns are accurately simulated by the model both for length and weight growth.

The parameterization performed recently by Stadnicka et al. (2018) is different from ours regarding both parameter values and modeled life-history. Stadnicka et al. (2018) used a different approach to account for sexual dimorphism. As explained above, we chose not to introduce differences in energy uptake behavior in order to avoid having consequences of a differential ability to cope with food scarcity in our IBM results. Moreover, we did not find observations in the literature of a different surface-specific assimilation rate for males and females. Finally, our parametrization provided a parameter set that enabled us to model sex-specific length and weight that corresponded well with empirical data from the wild (MNPCA data, see part 3.2.1) and in the laboratory at SCSU (Heiko Schoenfuss Lab, personal communication).

3.2 IBM parameterization

3.2.1 Parameterization of the different system types

We ensured that the systems that we analyzed were ecologically realistic by selecting those that followed a pattern of observed literature data.

First, we explored a parameter space of possible systems. We ran 20 replicates of each simulation. A simulation has a specific combination of four parameters:

Table SI-2.3: Comparison of our estimated parameters with the online values for parameter estimation (Stadnicka et al., 2018) for *Pimephales promelas*.

Symbol	Our Values	Online AMP Values	Units	Definition
	Primary parameters			
$[\dot{p}_M]$	133.5	334.791	J· cm^{-3}· d^{-1}	Volume-specific somatic maintenance rate
$\{\dot{p}_T\}$	0	0	J· cm^{-2}· d^{-1}	Surface-area-specific somatic maintenance rate
$[E_G]$	5228	5899.47	J· cm^{-3}	Volume-specific cost for structure
$\dot{v}$	0.01921	0.042512	cm· d^{-1}	Energy conductance
κ	0.4835	0.93255		Fraction reserve used for growth + maintenance
$\dot{k}_J$	0.0020	0.0020	d^{-1}	Maturity maintenance rate coefficient
E_H^b	0.722	0.228	J	Maturity threshold at birth
E_H^j	2.941	62.91	J	Maturity threshold at metamorphosis
E_H^p	3432	688.4	J	Maturity threshold at puberty
κ_R	0.95	0.95		Fraction of the reproduction buffer fixed into eggs
	Auxiliary and compound parameters			
T_A	8000	8000	K	Arrhenius temperature
T_{ref}	293.15	293.15	K	Temperature
δ_M	0.1268	0.21054		shape coefficient
z	0.6408	0.20018		Zoom factor for female
z_m	0.6408	0.26843		Zoom factor for male

Table SI-2.3: Comparison of our modeled data with the online estimated data values (Stadnicka et al., 2018) for *Pimephales promelas*.

Data (dimension)	Online AMP Value	Our Value
Age at birth (d)	5.069	5.926
Age at puberty for female (d)	90.12	133.7
Age at puberty for male (d)	90.12	111.9
Age at death (d)	1821	1460
Weight at birth (10^{-4} g)	6.216	3.548
Weight at puberty (g)	0.8122	0.7371
Weight at death for female (g)	2.043	3.077
Weight at death for male (g)	4.926	5.123
Length at birth (cm)	0.3652	0.3884
Length at puberty (cm)	3.993	4.931
Length at death for female (cm)	5.43	7.941
Length at death for male (cm)	7.281	9.411
Number of egg per day ($\#/d$)	12.53	33.12

- Intrinsic growth rate::

  $a_E \in [0.4, 0.8, 1.5]$;

- Carrying capacity:

  $k_E \in [500.00, 1000.0, 2000.0, 3000.0, 4000.0]$;

- Juvenile annual survival rate:

  $asr_J \in [0.005, 0.01, 0.025, 0.05, 0.1]$;

- Adult annual survival rate:

  $asr_A \in [0.4, 0.6, 0.8]$.

The total number of simulations was thus 4500. The number of selected sets of parameters was 109 out of 225 possible. Each of the 109 selected sets of parameters represents in a different river system type.

We ensured system realism by aiming to reproduce the following patterns for the fathead minnow, based on literature data:

1. An average fish population (individuals between 1.5 and 9.8 cm) density of 1-16 individuals per m^{-2} based on the Minnesota Pollution Control Agency (MPCA) Biological Monitoring Program (Fig. SI-2.4), https://www.pca.state.mn.us/water/biological-monitoring-water-minnesota;

2. An average of 14-26 reproduction events per female per year (Gale and Buynak, 1982);

3. An average female spawning interval (average time between reproduction events) between 2.5 and 5.5 days (Watanabe et al., 2007; Jensen et al., 2001);

4. An average clutch size between 80 and 140 eggs (Watanabe et al., 2007; Ankley et al., 2001).

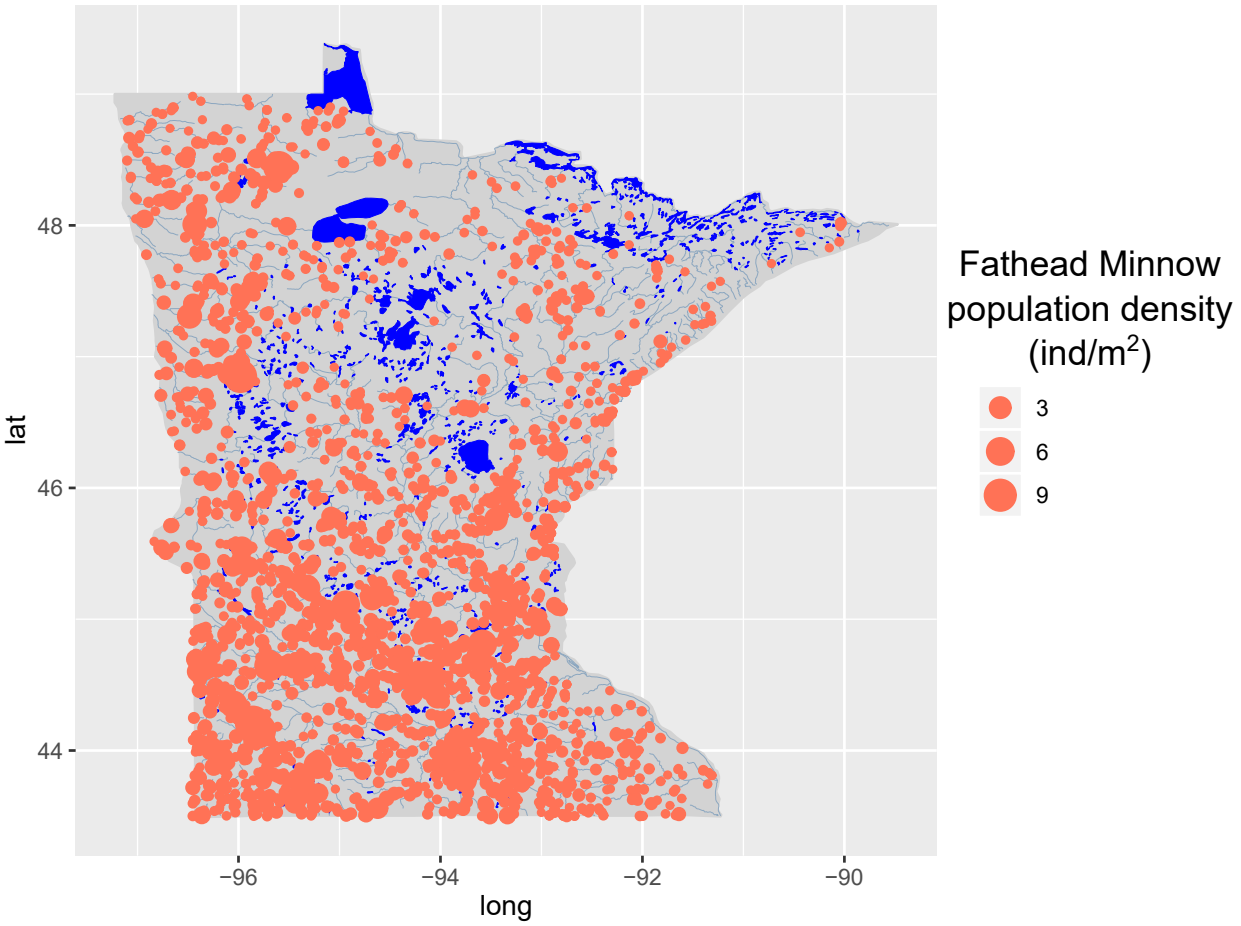

Figure SI-2.4: Fathead minnow (*Pimephales promelas*) population density in Minnesota. Minimum size limit is 1.5 cm and maximum size limit is 9.8 cm. Fish were collected by electro-fishing. Data obtained from the Minnesota Pollution Control Agency (MPCA) Biological Monitoring Program, https://www.pca.state.mn.us/water/biological-monitoring-water-minnesota.

4 Conceptual model evaluation

This TRACE element provides supporting information on: The simplifying assumptions underlying a model's design, both with regard to empirical knowledge and general, basic principles. This critical evaluation allows model users to understand that model design was not ad hoc, but based on carefully scrutinized considerations.

Summary:

Consideration of modeled metabolic processes was based on Dynamic Energy Budget theory that postulates how resources are assimilated and allocated to metabolic processes. It is based on first principles of conservation of energy, matter, isotopes and time, and follows strict assumptions of how energy fluxes are distributed in the organism.

The conceptual model is based on DEB theory (Figure SI-2.1), which is also described under 3.1.1. The scheduling of processes and events is described in 2.3.

5 Implementation verification

This TRACE element provides supporting information on: Whether the computer code implementing the model has been thoroughly tested for programming errors, whether the implemented model performs as indicated by the model description, and how the software has been designed and documented to provide necessary usability tools (interfaces, automation of experiments, etc.) and to facilitate future installation, modification, and maintenance.

Summary:

Model implementation was verified in a series of tests to ensure that the code reproduced the concepts described in sections 2.3 and 2.4. Verification was performed using modeling platform tools for syntax checking, in addition to visual testing, print statements, spot testing with agent monitors, stress tests, test programs, and code reimplementation.

Model code was tested to verify that the model behaves as expected and as planned. The model was implemented in Java, and parts were implemented using Matlab (MATLAB R2016b) or R (R Core Team 2017). All of these languages offer several tools that enable the developer to check whether the implemented syntax is correct.

Implementation testing was done on several levels:

1. Syntax checking. Using software tools, which check for syntax errors such as forgetting a bracket. These errors are immediately picked up by the software without a possibility to proceed with simulations until the syntax has been corrected. Run-time errors are not syntax errors, but represent events that the software cannot deal with. This, for instance, includes divisions by zero or producing numbers that are too large for storing. Even though run-time errors cannot directly pinpoint to the problem, they offer helpful directions and explanations of the issue.

2. Visual testing of model outputs. Visual testing was continuously used to look for errors that may be unlikely to be detected soon, if ever, via other methods. Individual energy fluxes and properties (*e.g.*, length, number of eggs, reproduction period) and overall population dynamics

have all been monitored for checking whether the model behaves as expected. For instance, modeled fluxes have been controlled for equilibrium, the energy entering the organism being equal to the energy used and excreted by the organism. Food levels have been adjusted to avoid frequent extinctions, and recruitment has been adjusted to avoid the death of too many adults by starvation.

3. Print statements. Using the print statements allowed for a visual check and manual calculation of the correct functioning of all submodels. We programmed the model to print the value of some variables at different times to check that the model was behaving as expected. Basic examples are: writing the number of agents at every time step to check that they are actually dying and leaving the model; writing some particular energy values (such as energy at birth); write the time of a specific event, *e.g.*, reproduction. Print statements were also used to locate issues such that they would have a role of markers in the code, *e.g.* if not printed, that meant that the code lines were not reached or a particular error was (not) made.

4. Spot tests with Agent Monitors. The agent monitors were used to quickly view agent state variable values, and test key calculations such as transitions between life stages, age and length measurements.

5. Stress tests. Stress tests were performed using extreme values of parameters and comparing simulation outputs to expectations. For example, food availability or temperature were changed to study both individual and population levels dynamics; reproduction-related parameters were shut off to check population dynamics.

6. Test programs. In some cases, a separate, short program under simplified conditions was written to test a particular algorithm or procedure. For instance, the temperature implementation and calculation of the shape correction factor were first done in a secondary program.

7. Simulations experiments. Several controlled simulation experiments were performed in which the model or its parts were simplified so that the outcome of each experiment could be predicted and verified. This includes, for example, the different mortality submodels.

8. Code reviews. The code was peer-reviewed, *i.e.*, it was thoroughly compared with the written formulation of the model by one other scientist and with published DEB-IBMs.

6 Model output verification

This TRACE element provides supporting information on: How well model output matches observations, and how much calibration and effects of environmental drivers were involved in obtaining good fits of model output and data.

Summary:

Here we summarize how well the model recreates the input data. This includes data on length, weight, the resulting number of eggs per reproductive event, the number of reproductive events, the spawning interval, and fish population density.

6.1 Individual scale

We ran IBM simulations of 10,000 individuals with unlimited food, no predation, and constant temperature to compare outputs with those of the DEB model parameterization (Table SI-2.1 and Figures SI-2.2 and SI-2.3 in 3.1). Comparison between IBM outputs and DEB model parameterization outputs for zero-variate data (Table SI-2.4) show similar results.

Growth curves in length and weight obtained with the IBM simulation for females (Figure SI-2.5) and males (Figure SI-2.6) were similar to those obtained during DEB parameterization (Figures SI-2.2 and SI-2.3, respectively). Whereas all figures showed a part of the growth that seems erratic (and even decreasing), loss of length is not possible in the IBM. These patterns are only observed because we measure the average daily length (or weight) of a cohort that is decreasing in size because some individuals are dying of aging.There are fewer individuals near the end of the simulation, which makes the size measurements more variable from day to day.

Table SI-2.4: Modeled data with the IBM versus modeled data during the parameter estimation of DEB model for *Pimephales promelas*.

Data (dimension)	Modeled with IBM	Modeled with DEB model
Age at hatching (d)	6	4.801
Age at hatching at 15 °C (d)	14	12.18
Age at birth (d)	8	5.926
Age at puberty for females (d)	137	133.7
Age at puberty for males (d)	118	111.9
Age at death (d)	1379	1460
Wet weight at birth (10^{-4} g)	3.8	3.602
Wet weight at puberty for females (g)	0.676	0.7371
Wet weight at puberty for males (g)	0.834	0.8514
Wet weight at death for females (g)	3.365	3.077
Wet weight at death for males (g)	5.294	5.123
Length at birth (cm)	0.422	0.3884
Length at puberty for females (cm)	4.782	4.931
Length at puberty for males (cm)	5.137	5.174
Length at death for females (cm)	8.104S	7.941
Length at death for males (cm)	9.431	9.411
Number of eggs per day ($\#/d$)	30.76	33.12

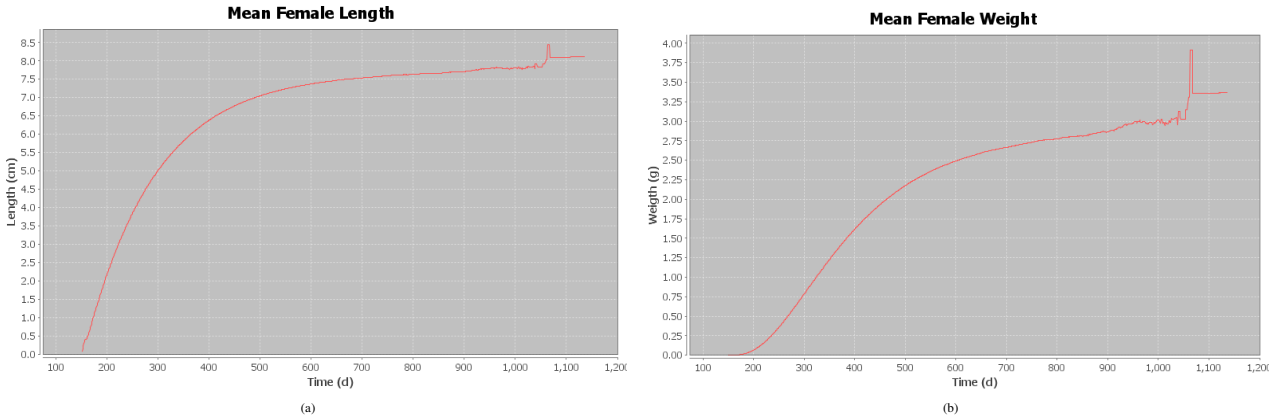

Figure SI-2.5: IBM modeled length (a) and weight (b) for female *Pimephales promelas*.The red line represents the average of 10,000 individuals.

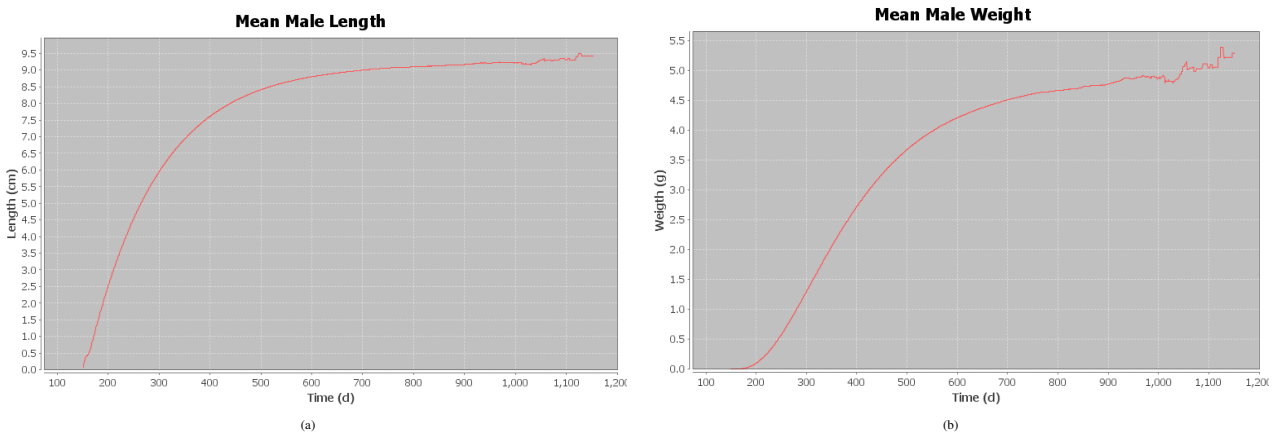

Figure SI-2.6: IBM modeled length (a) and wet weight (b) for male *Pimephales promelas*. The red line represents the average of 10,000 individuals.

6.2 Population scale

We explored many possible systems, and selected the ones that produced realistic patterns according to the published literature (see 3.2.1). The distributions of the average fish density (Figure SI-2.7), the average number of reproductive events per female (Figure SI-2.8), the average spawning interval per female (Figure SI-2.9) and the average number of eggs per clutch (Figure SI-2.10) for all the systems modeled demonstrate that the population-level outputs were realistic.

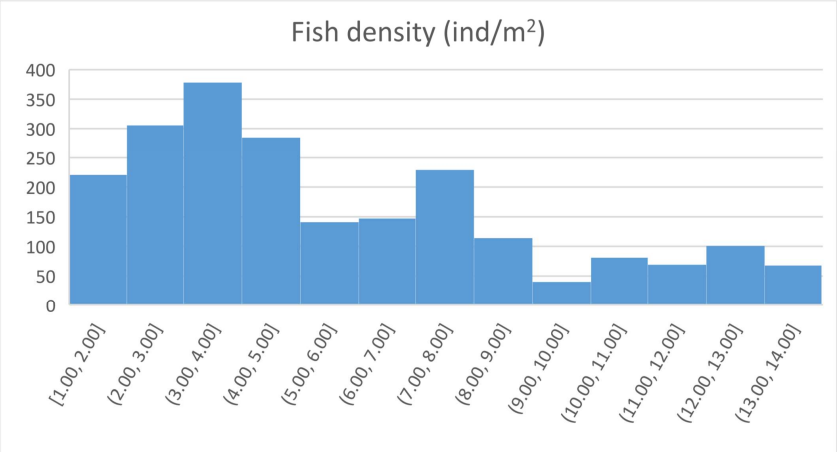

Figure SI-2.7: The distribution of the IBM modeled average fish density (*Pimephales promelas*) for all of the 109 selected systems. x-axis is fish density and y-axis the frequency.

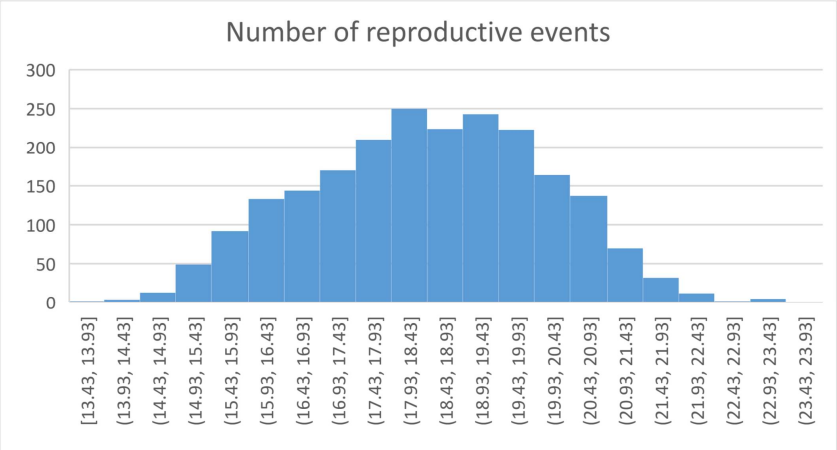

Figure SI-2.8: The distribution of the IBM modeled average number of reproductive events per female (*Pimephales promelas*) for all of the 109 selected systems. x-axis is the average number of reproductive events per female and y-axis the frequency.

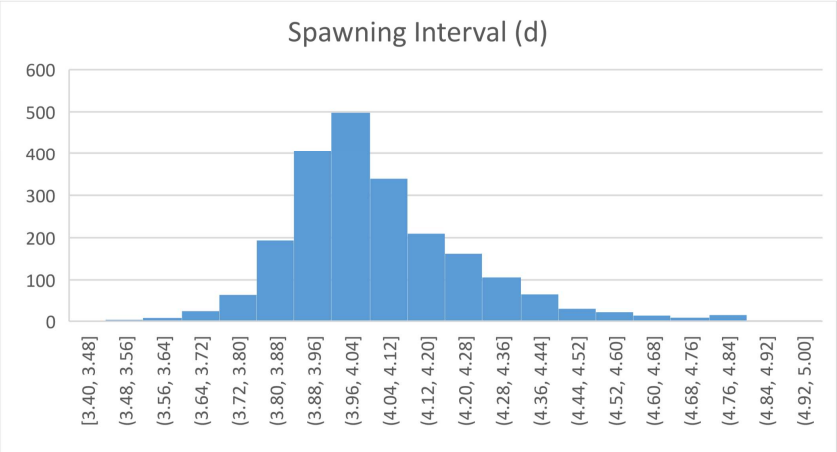

Figure SI-2.9: The distribution of the IBM modeled average spawning interval per female (*Pimephales promelas*) for all of the 109 selected systems. x-axis is the average spawning interval per female and y-axis the frequency.

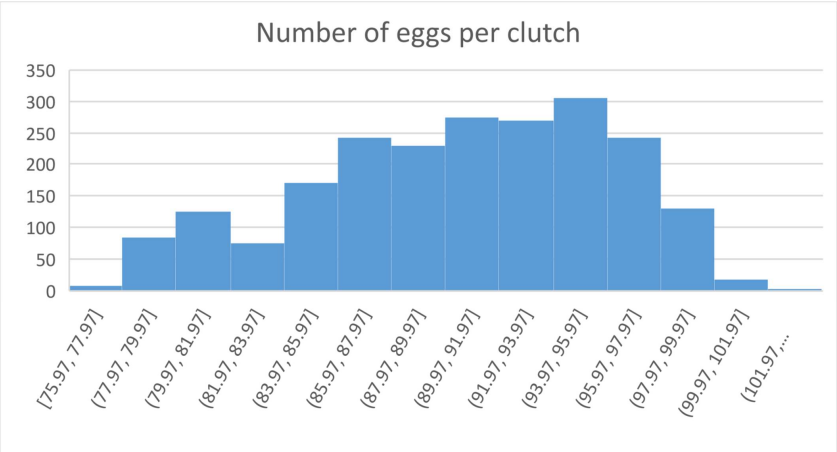

Figure SI-2.10: The distribution of the IBM modeled average number of eggs per clutch per female (*Pimephales promelas*) for all of the 109 selected systems. x-axis is the average number of eggs per clutch per female and y-axis the frequency.

7 Model analysis

This TRACE element provides supporting information on: How sensitive model outputs are to changes in model parameters (sensitivity analysis), and how well the emergence of model outputs has been understood.

Summary:

In this section, we present the results of sensitivity analysis and an analysis of the different system types. We also justify the choice of the number of replicates.

7.1 Number of replicates and total number of simulations

We did 20 replicates of each simulation because the value of the average population size was stable from 10 to 20replicates (Figure SI-2.11). A total of 4,500 simulations were analyzed when selecting the different systems (see 3.2.1). We analyzed how four different PMoAs at four different levels impacted 109 different systems. In total, we analyzed 45,780 simulations (including 2,180 simulations with no effects) in this study.

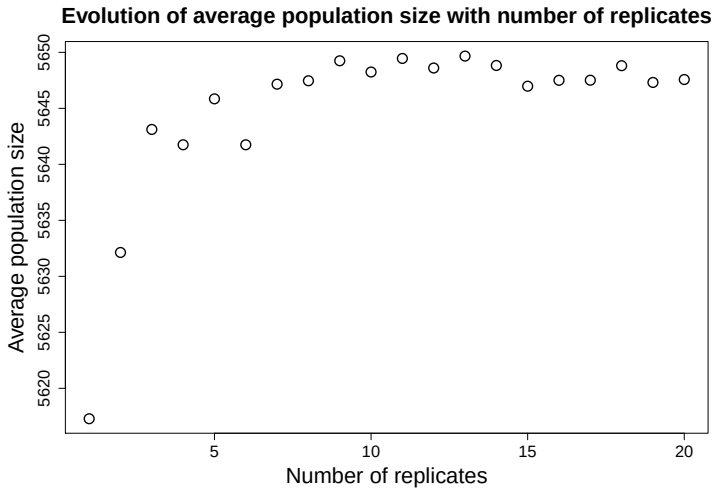

Figure SI-2.11: The relationship between average *Pimephales promelas* population size change and the number of replicates.

7.2 Sensitivity analysis

The aim of our study was to infer population-level effects in systems in which population size is controlled by different combinations of food availability and predation pressure. Analyses of the different systems is provided in section 7.3, which shows how population size and biomass change with changing food and predation parameters.

We conducted sensitivity analyses that considered a ±10% variation of DEB parameter values. To conduct this sensitivity analysis, we randomly selected 5 systems with a Starvation Index < 0.05, and 5 systems with a Starvation Index ≥ 0.05. We selected this threshold value of Starvation Index based on the results of the study highlighting that response to a stressor was different below and above this value. The changes in population size and biomass were calculated as:

$$\Delta Obs = \sum_{i=1}^{n} \frac{\overline{Obs_i} - \overline{Obs_{ref}}}{\overline{Obs_{ref}}} * 100,$$

where $\overline{Obs_{ref}}$ is the average population size or biomass of 20 simulations with no effects of stressors and the original set of parameters, and $\overline{Obs_i}$ is the average population size or biomass of 20 simulations with no effects of stressors and a modified set of parameters (±10% on the value of one parameter) for a system i.

Overall, the model is not very sensitive to most parameters except for the parameter z when Starvation Index is < 0.05.

The systems with a Starvation Index ≥ 0.05 were more sensitive to a change in parameter values for biomass than for population size (Table SI-2.11). The parameter that impact the most the population size is $delta_M$ whereas the parameters that impact biomass the most are $\dot{v}$, z, κ, E_H^b, E_H^j, E_H^{jm}, and E_H^p.

The systems with a Starvation Index < 0.05 were more sensitive to a change in parameter value for population size than for biomass (Table SI-2.11). The parameters that impact biomass the most are z and E_H^{jm}, whereas the parameters that impact population size the most are z, κ, E_H^b, E_H^j, E_H^j and $delta_M$.

The model was sensitive to changes in the zoom factor z only for decreases in population biomass in systems with a small Starvation Index. In a DEB model, the zoom factor impacts the maximum specific assimilation rate $\{\dot{p}_{Am}\}$ and by consequence the maximum length, as well as the life-stage

Table SI-2.11: Sensitivity analysis of DEB parameters for large (≥ 0.05) Starvation Index systems. For each line, we changed the value of the corresponding parameter by + and - 10 % and we measured the change in population size and biomass compared to simulations with unchanged parameter value.

Symbol	Our Values	±10% values	$\Delta_{population\ size}$ (%)	$\Delta_{population\ biomass}$ (%)
z	0.6408	0.70488 ; 0.57672	-2.62 ; 2.47	2.13 ; -8.29
$[\dot{F}_m]$	6.5	7.15 ; 5.85	-4.46 ; 4.96	-3.31 ; 2.04
$\dot{v}$	0.01921	0.021137 ; 0.017289	-2.48 ; 2.25	-14.36 ; 10.04
κ	0.4835	0.5291 ; 0.4329	-5.32 ; 2.22	-1.10 ; -9.24
$[\dot{p}_M]$	133.5	146.85 ; 120.15	-3.13 ; 4.26	-3.42 ; -0.96
$[E_G]$	5228	5750.8 ; 4705.2	0.22 ; -0.94	-3.94 ; -2.85
E_H^h	0.722	0.53185 ; 0.43515	0.81 -0.12	-4.43 ; -0.68
E_H^b	0.722	0.7945 ; 0.64.98	1.09 ; -2.90	3.20 ; -12.67
E_H^j	2.941	3.2351 ; 2.6469	2.78 ; -4.84	-14.87 ; 12.58
E_H^p	3432	3775.2 ; 3088.8	-3.92 ; 4.13	7.75 ; -12.51
E_H^{jm}	4.927	5.4197 ; 4.4343	-5.02 ; 5.75	11.13 ; -12.36
E_H^{pm}	3491	3840.1 ; 3141.9	1.02 ; -1.68	-9.17 ; 9.02
δ_M	0.1268	0.13948 ; 0.11412	-11.61 ; 12.16	-1.70 ; -0.48
T_A	8000	8800 ; 7200	-1.67 ; 1.17	-4.83 ; -1.01

parameters (E_H^b, E_H^j and E_H^p). An increase in z results in a higher $\{\dot{p}_{Am}\}$, leading to an increase of the maximum reserve capacity and of the contribution of reserve to weight (Lika et al. (2011); Kooijman (2010)).

The model is also sensitive to the energy conductance $\dot{v}$, but only for biomass and for systems with a large Starvation Index. This parameter controls the reserve mobilization. A high value gives a high growth rate, short development time to reach birth or maturity, a low maximum reserve density, and lower resistance to starvation.

The model was sensitive to changes in κ (fraction of mobilized energy to soma) only for increases in population size in systems with a small Starvation Index. A high κ value results in very little reserve allocated to maturation/development and reproduction, and therefore a reduction in individual length and weight. Conversely, a low κ means more energy allocated to development and reproduction.

The model was sensitive to changes in four life-history thresholds (E_H^b, E_H^{jm}, E_H^j and E_H^p) in systems with both a low and high Starvation Index. Sensitivity of population biomass was greater in systems with a high Starvation Index, whereas sensitivity of population size was greater in systems with a low Starvation Index. E_H^b, E_H^{jm} and E_H^j affect the calculation of the shape correction function (sc) (see

2.13) which thus impacts growth and reproduction. E_H^p controls the start of the adult stage, and thus impacts the population recruitment. Moreover, all of these life-history thresholds impact the overall population mortality due to predation because they determine the duration of each life stage.

Table SI-2.11: Sensitivity analysis of DEB parameters for small (< 0.05) Starvation Index systems. For each line, we changed the value of the corresponding parameter by + and - 10 % and we measured the change in population size and biomass compared to simulations with unchanged parameter value.

Symbol	Our Values	±10% values	$\Delta_{population\ size}$ (%)	$\Delta_{population\ biomass}$ (%)
z	0.6408	0.70488 ; 0.57672	2.90 ; -21.76	7.52 ; -24.21
$[\dot{F}_m]$	6.5	7.15 ; 5.85	1.01 ; -5.91	3.03 ; -5.87
$\dot{v}$	0.01921	0.021137 ; 0.017289	0.93 ; -7.32	-5.67 ; 5.12
κ	0.4835	0.5291 ; 0.4329	-18.36 ; 5.62	-8.67 ; -4.03
$[\dot{p}_M]$	133.5	146.85 ; 120.15	-2.04 ; -5.18	-1.47 ; -3.45
$[E_G]$	5228	5750.8 ; 4705.2	-3.05 ; 2.33	-3.88 ; 3.07
E_H^h	0.722	0.53185 ; 0.43515	2.20 ; -2.76	-2.45 ; 1.19
E_H^b	0.722	0.7945 ; 0.64.98	-13.54 ; 5.60	-5.13 ; -1.39
E_H^j	2.941	3.2351 ; 2.6469	7.23 ; -14.27	-5.46 ; 2.55
E_H^p	3432	3775.2 ; 3088.8	-11.17 ; 7.28	2.14 ; -4.07
E_H^{jm}	4.927	5.4197 ; 4.4343	-5.05 ; 4.82	10.51 ; -9.33
E_H^{pm}	3491	3840.1 ; 3141.9	0.01 ; -1.08	-5.7 ; 8.77
δ_M	0.1268	0.13948 ; 0.11412	-11.44 ; 10.99	-0.14 ; 1.13
T_A	8000	8800 ; 7200	-5.38 ; 7.25	-5.17 ; 5.1

7.3 Analysis of the different system types

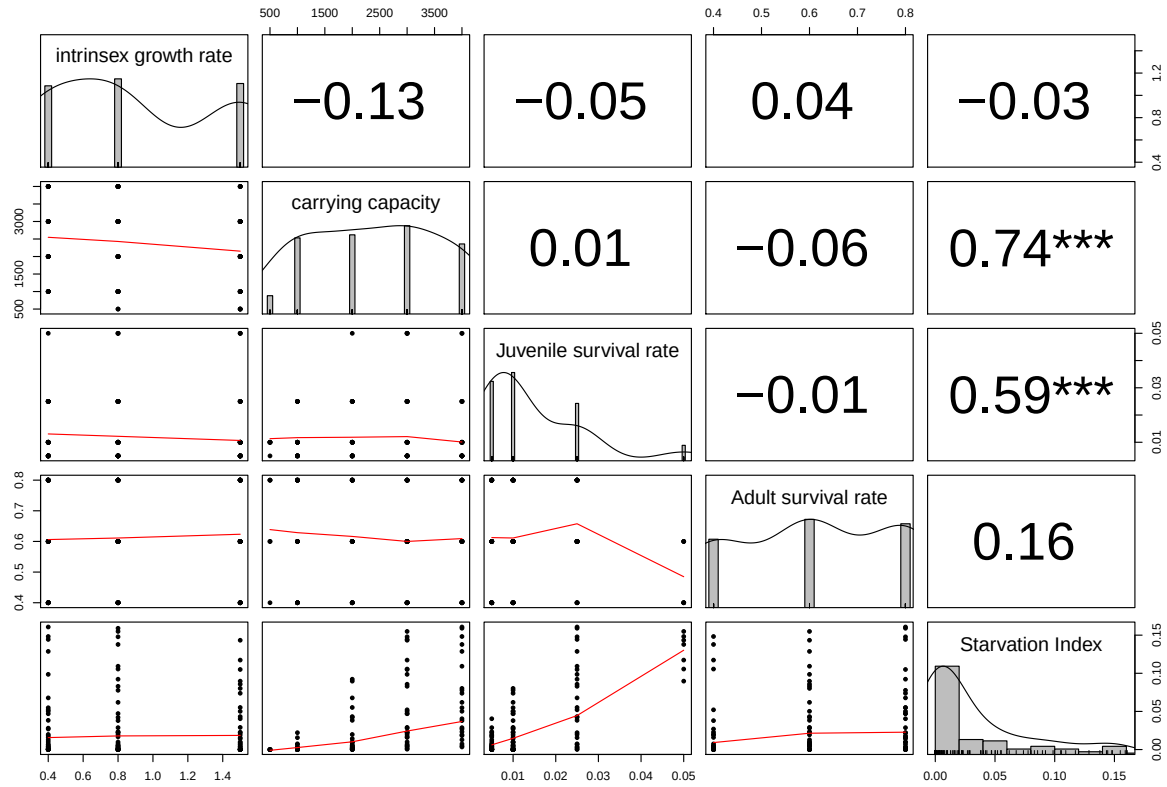

Figure SI-2.12: A scatter plot of matrices showing how environmental parameters are correlated and how they correlate to the Starvation Index. Bivariate scatter plots are below the diagonal, histograms on the diagonal, and the Pearson correlation above the diagonal.

Figures SI-2.12, SI-2.13 and SI-2.14 provide a description of the different systems selected. We calculated a Starvation Index to scale the different systems from predation-controlled (Starvation Index close to zero) to food-controlled (higher Starvation Index). The Starvation Index is calculated as the number of individuals that died from starvation divided by the total number of dead individuals. Figure SI-2.12 indicates that there are no strong correlations with the Starvation Index neither for the intrinsic growth rate a_E (-0.03), nor the adult annual survival rate asr_A (0.16). The juvenile annual survival rate (asr_J, 0.59) and the carrying capacity (k_E 0.74) show a stronger correlation with the Starvation Index.

Population size (0.64) and population biomass (0.65) are slightly correlated with the Starvation Index (Fig. SI-2.13). Population Size Distribution (PSD, 0.73) is more importantly positively correlated

with the Starvation Index whereas the K index (-0.70) is negatively correlated with the Starvation Index.

The number of eggs per clutch (0.03), the number of reproduction events (-0.25), and the spawning interval (-0.06) are not correlated with the Starvation Index (Fig. SI-2.14).

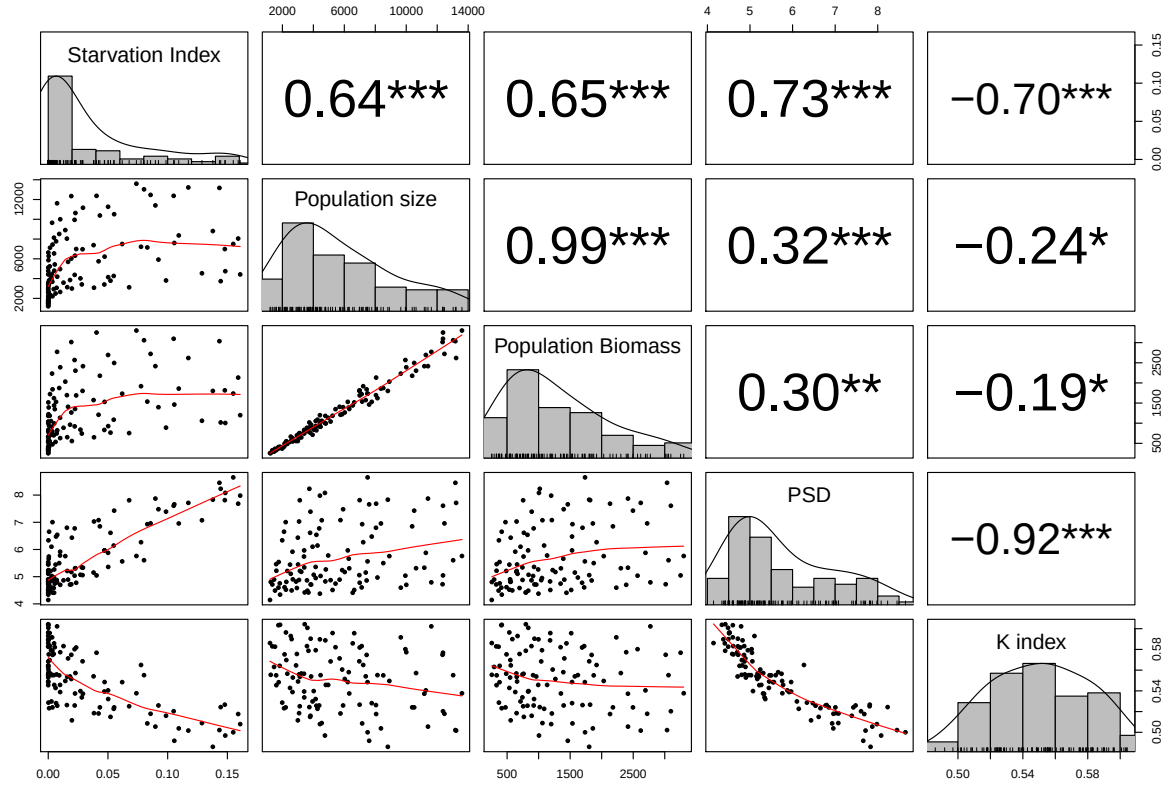

Figure SI-2.13: Histograms of each modeled population outputs (diagonal), and scatterplots of the association between each of the modeled output and the Starvation Index with corresponding Spearman correlation coefficients.

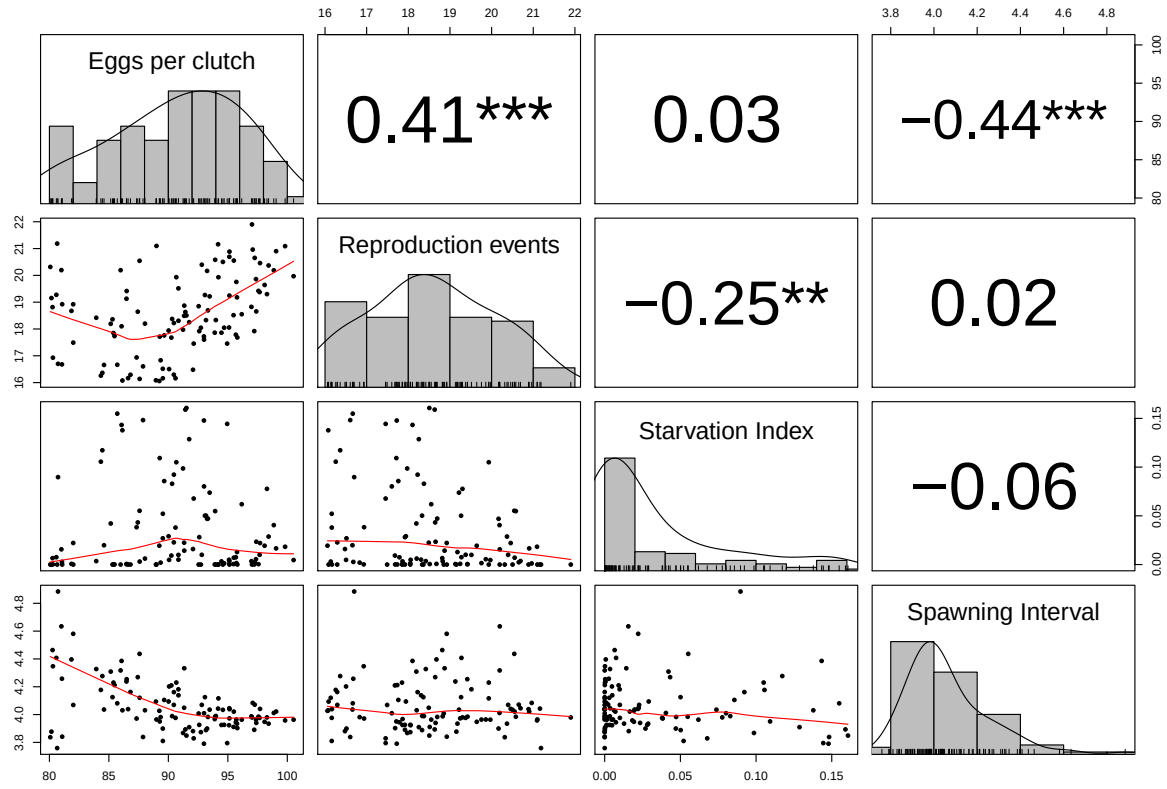

Figure SI-2.14: Histograms of each modeled population outputs (diagonal), and scatterplots of the association between each of the modeled output and the Starvation Index with corresponding Spearman correlation coefficients.

7.4 Per capita population growth rate

In this study, we calculated the daily per capita growth rate (PCGR) as the daily change in total biomass of individuals between 1.5 and 9.8 cm, divided by the number of individuals in this size range. This standard measure allowed us to compare population growth rate across different combinations of predation and food control (*i.e.*, different population sizes). We linked the PCGR to different intervals of population density (20 intervals, population density ranging from0 to 10,000) according to the population density on the day of the computation. We found that the relationship was convex for all systems regardless of whether they had a large or small starvation index (Figure SI-2.15).

We linearized these relationships by log transformation. Then, we fitted the following logarithmic

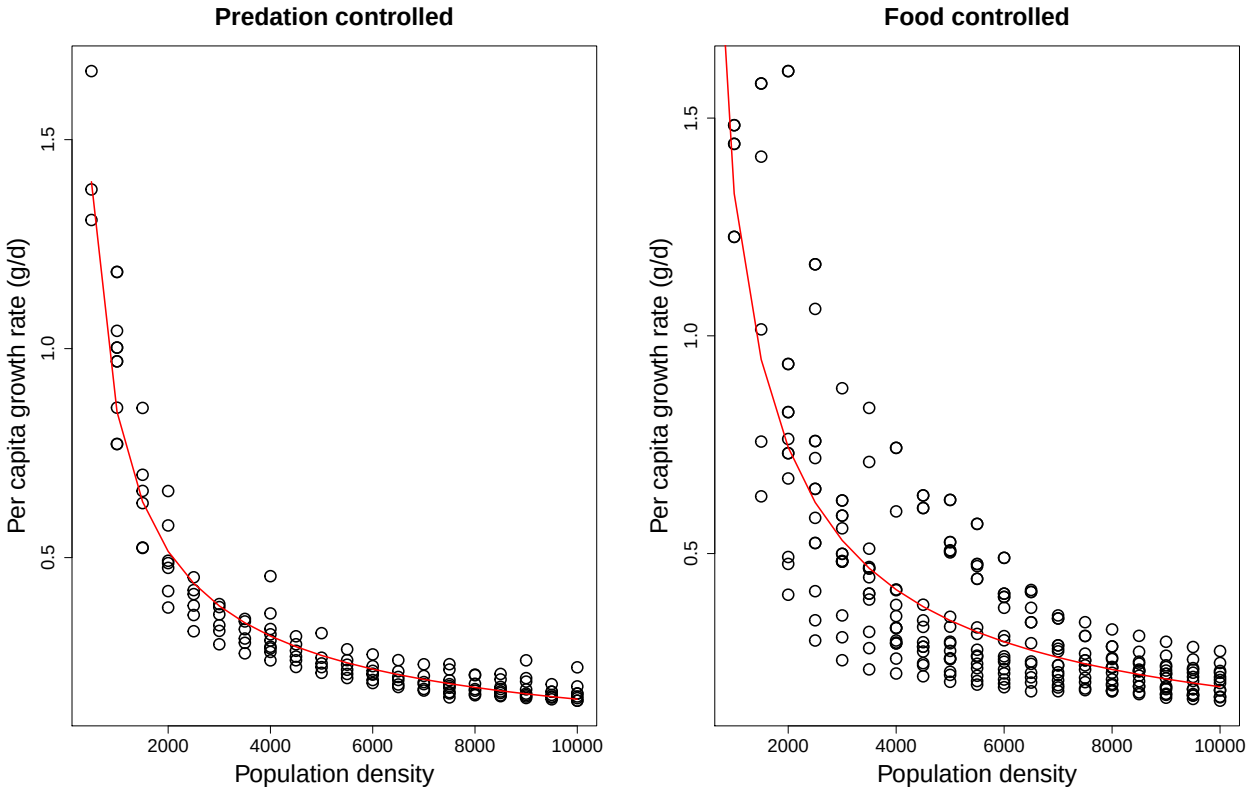

Figure SI-2.15: Per capita growth rate (PCGR) as a function of population size in predation-controlled systems (Starvation Index lower than 0.001) (a), and in food-controlled systems (Starvation Index larger than 0.1) (b).

function with a linear regression using the R function "lm()" with default arguments option:

$$log(PCGR) = A + DD_s * log(FD),$$

where FD is fish population density. A was estimated for every system, but was held constant when comparing exposed and non-exposed systems. DDs, which represents the strength of density-dependence, was estimated for every system and exposure condition. The underlying idea was that exposure would change the strength of the density dependence only.

Results showed that density-dependence was impacted by stressors in different ways depending on the PMoA involved, and whether the system was predation- or food-controlled (Figure SI-2.16). An increase in the value of DD_s increases the curvature (curve becomes more convex) of the PCGR relationship with population size. In the figure 7 of the main paper, we related the change in curvature

to population size change and Starvation Index.

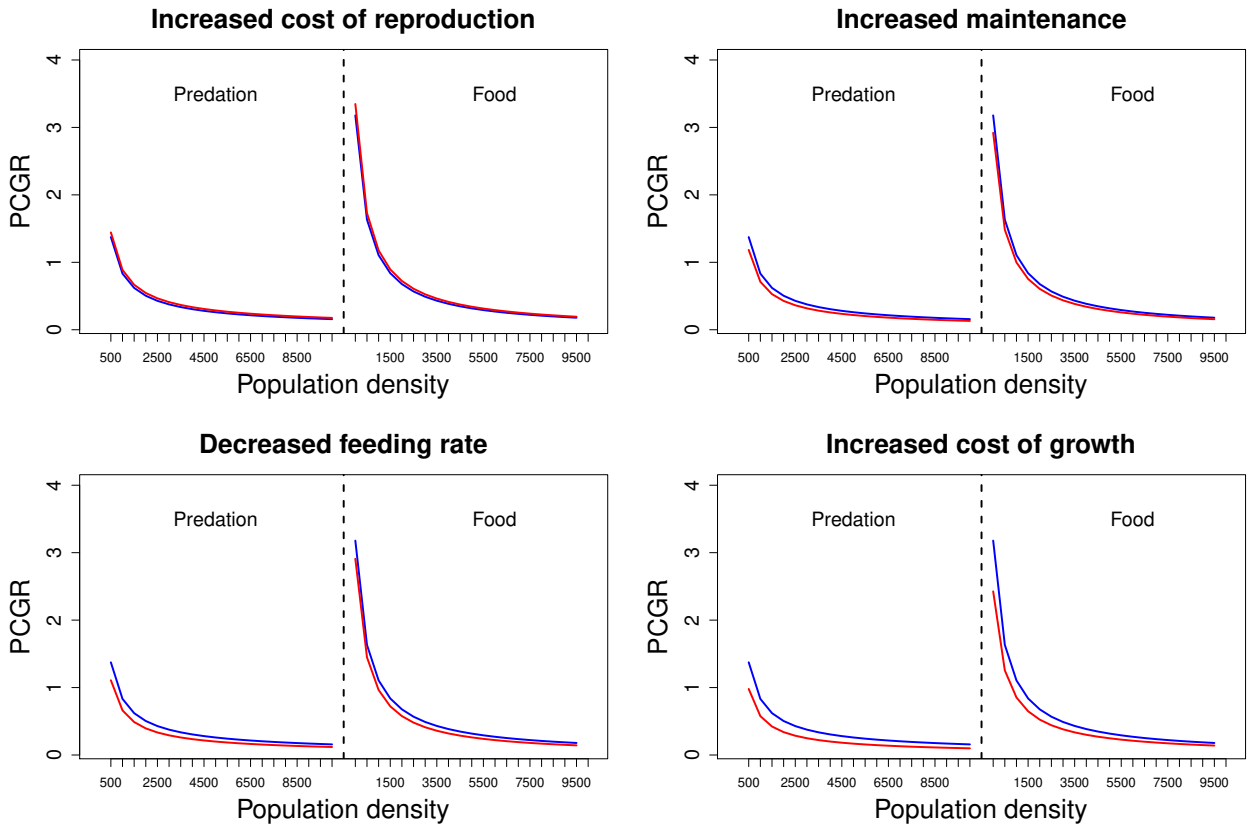

Figure SI-2.16: Per capita growth rate (PCGR) as a function of population size in predation-controlled systems (Starvation Index lower than 0.001), and in food-controlled systems (Starvation Index larger than 0.1). Blue lines are PCGR when systems are not impacted by stressor and red lines are PCGR when systems are impacted by a stressor. The PMoA of a stressor can either be on Assimilation, Maintenance, Feeding rate, or Growth.

8 Model output corroboration

This TRACE element provides supporting information on: How model predictions compare to independent data and patterns that were not used, and preferably not even known, when the model was developed, parameterized, and verified. By documenting model output corroboration, model users learn about evidence which, in addition to model output verification, indicates that the model is structurally realistic so that its predictions can be trusted to some degree.

Summary:

Our model has not been compared to independent data. The individual-level outputs were compared to literature data during DEB model parameterization (see 3.1). All of the 109 systems modeled with the IBM were selected based on a pattern defined by literature data. This process is detailed in 3.2.1.

Our model is a theoretical study, based on the strong assumptions of DEB theory. The individual-level processes in the model are based on published DEB outputs, and our model outputs provide good fits to observed values (see 3.1).

Stressor effects are hypothetical but represent realistic physiological mechanisms by which stressors may affect the metabolism of organisms. Qualitatively our results are similar to other model outputs found in the literature (as explained in the Discussion section of the main study). Because population dynamics are very few and because we simulated multiples systems, a comparison with independent data has not been possible so far. However, we ensured that the systems modeled in our study were all realistic by comparing some of the IBM outputs (Population density, spawning interval, number of reproductive events and eggs per clutch per female) to literature data (this process is detailed in 3.2.1).

References

Álvarez, O.A., Jager, T., Redondo, E.M., Kammenga, J.E., 2006. Physiological modes of action of toxic chemicals in the nematode acrobeloides nanus. Environmental Toxicology and Chemistry 25, 3230–3237.

Andrews, A., Flickinger, S., 1974. Spawning requirements and characteristics of the fathead minnow, in: Proc Southeast Assoc Game Fish Comm, pp. 759–766.

Ankley, G.T., Jensen, K.M., Kahl, M.D., Korte, J.J., Makynen, E.A., 2001. Description and evaluation of a short-term reproduction test with the fathead minnow (*Pimephales promelas*). Environmental toxicology and chemistry 20, 1276–1290.

Braunbeck, T., Streit, B., Hinton, D.E., 1998. Fish ecotoxicology. Basel ; Boston : Birkhä user Verlag.

Cox, M., Peterson, K., Tan, D., Novak, P.J., Schoenfuss, H., Ward, J., 2018. Temperature modulates estrone degradation and biological effects of exposure in fathead minnows. Science of the Total Environment 621, 1591–1600.

Dumoulin, N., 2007. Simaqualife: un cadriciel pour la modelisation de la dynamique spatiale d'organismes aquatiques. TSI. Technique et science informatiques 26, 701–721.

Etnier, D.A., Starnes, W.C., 1993. The fishes of Tennessee. University of Tennessee Press.

Gale, W.F., Buynak, G.L., 1982. Fecundity and spawning frequency of the fathead minnow - a fractional spawner. Transactions of the American Fisheries Society 111, 35–40.

Grimm, V., Berger, U., Bastiansen, F., Eliassen, S., Ginot, V., Giske, J., Goss-Custard, J., Grand, T., Heinz, S.K., Huse, G., et al., 2006. A standard protocol for describing individual-based and agent-based models. Ecological modelling 198, 115–126.

Grimm, V., Berger, U., DeAngelis, D.L., Polhill, J.G., Giske, J., Railsback, S.F., 2010. The odd protocol: a review and first update. Ecological modelling 221, 2760–2768.

Jager, T., Zimmer, E., 2012. Making sense of chemical stress application of dynamic energy budget theory in ecotoxicology and stress ecology.

Jeffries, M.K.S., Stultz, A.E., Smith, A.W., Stephens, D.A., Rawlings, J.M., Belanger, S.E., Oris, J.T., 2015. The fish embryo toxicity test as a replacement for the larval growth and survival test: A comparison of test sensitivity and identification of alternative endpoints in zebrafish and fathead minnows. Environmental toxicology and chemistry 34, 1369–1381.

Jensen, K.M., Korte, J.J., Kahl, M., Pasha, M.S., Ankley, G.T., 2001. Aspects of basic reproductive biology and endocrinology in the fathead minnow (*Pimephales promelas*). Comparative Biochemistry and Physiology Part C: Toxicology & Pharmacology 128, 127–141.

Jusup, M., Sousa, T., Domingos, T., Labinac, V., Marn, N., Wang, Z., Klanjšček, T., 2016. Physics of metabolic organization. Physics of Life Reviews .

Kooijman, S.A.L.M., 2010. Dynamic energy budget theory for metabolic organisation. Cambridge university press.

Kooijman, S.A.L.M., Van der Hoeven, N., Van der Werf, D.C., 1989. Population consequences of a physiological model for individuals. Functional Ecology , 325–336.

Kooijman, S.A.L.M., Sousa, T., Pecquerie, L., Van der Meer, J., Jager, T., 2008. From food-dependent statistics to metabolic parameters, a practical guide to the use of dynamic energy budget theory. Biological Reviews 83, 533–552.

Korn, V., 2018. Effects of estrone and temperature on the predator-prey relationship between bluegill sunfish and fathead minnows. Culminating Projects in Biology 30. URL: `https://repository.stcloudstate.edu/biol_etds/30`.

Lika, K., Kearney, M.R., Freitas, V., van der Veer, H.W., van der Meer, J., Wijsman, J.W.M., Pecquerie, L., Kooijman, S.A.L.M., 2011. The "covariation method" for estimating the parameters of the standard dynamic energy budget model i: philosophy and approach. Journal of Sea Research 66, 270–277.

Martin, B.T., Zimmer, E.I., Grimm, V., Jager, T., 2012. Dynamic energy budget theory meets individual-based modelling: a generic and accessible implementation. Methods in Ecology and Evolution 3, 445–449.

van der Meer, J., 2006. An introduction to dynamic energy budget (deb) models with special emphasis on parameter estimation. Journal of Sea Research 56, 85–102.

Nisbet, R.M., Muller, E.B., Lika, K., Kooijman, S.A.L.M., 2000. From molecules to ecosystems through dynamic energy budget models. Journal of animal ecology 69, 913–926.

Shin, Y., Rochet, M., Jennings, S., Field, J., Gislason, H., 2005. Using size-based indicators to evaluate the ecosystem effects of fishing. ICES Journal of marine Science 62, 384–396.

Sommer, A., 2011. "*Pimephales promelas*" (on-line), animal diversity web. URL: http://animaldiversity.org/accounts/Pimephales_promelas/.

Sousa, T., Domingos, T., Poggiale, J.C., Kooijman, S.A.L.M., 2010. Formalised deb theory restores coherence in core biology. Phil. Trans. R. Soc. B 365, 3413–3428.

Stadnicka, J., Kooijman, S., Kuhl, R., Zimmer, E., 2018. Amp entry for *Pimephales promelas*. URL: https://www.bio.vu.nl/thb/deb/deblab/add_my_pet/entries_web/Pimephales_promelas/Pimephales_promelas_res.html.

Wang, J.C.S., 1986. Fishes of the Sacramento-San Joaquin estuary and adjacent waters, California: A guide to the early life histories. Technical Report. Citeseer.

Ward, J., Cox, M., Schoenfuss, H., 2017. Thermal modulation of anthropogenic estrogen exposure on a freshwater fish at two life stages. Hormones and behavior 94, 21–32.

Watanabe, K.H., Jensen, K.M., Orlando, E.F., Ankley, G.T., 2007. What is normal? a characterization of the values and variability in reproductive endpoints of the fathead minnow, *Pimephales promelas*. Comparative Biochemistry and Physiology Part C: Toxicology & Pharmacology 146, 348–356.